Ab initio calculations for medium-mass nuclei and electromagnetic observables

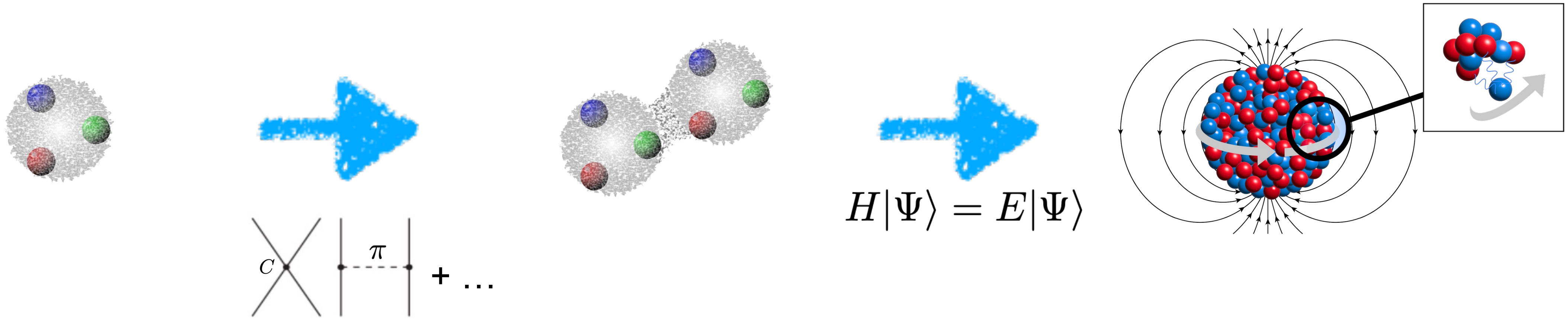

ERATO TOMOE

Takayuki Miyagi

Low-Energy Electron Scattering for Nucleon and Exotic Nuclei @ Tohoku University (Oct. 31, 2024)

Collaborators

TU Darmstadt: C. Brase, K. Hebeler, A. Schwenk, R. Seutin

TRIUMF: J. D. Holt

University of Illinois: X. Cao

Massachusetts Institute of Technology: R. G. Ruiz

Johannes Gutenberg University of Mainz: S. Bacca

University of Barcelona: J. Menendez

IJCLab: P. Arthuis

ORNL: M. Heinz

Motivations

筑波大学 計算科学研究センター Center for Computational Sciences

EM observables can be used

- to investigate nuclear structure (shell structure, shape, …)
- to test theories

To test our theories, we need:

- (precise) experimental data
- reasonable starting nuclear Hamiltonian(s)
- controllable many-body method(s)
- higher-order contribution of EM operators (main focus of this talk)

$$H|\Psi\rangle = E|\Psi\rangle$$

$$O_{\mathrm{EM}}^{\mathrm{exp.}} \sim \langle\Psi|\mathcal{O}_{\mathrm{EM}}|\Psi\rangle$$

Motivations

Magnetic dipole moment: $$\langle \mu \rangle = \sqrt{\frac{J}{(J+1)(2J+1)}} \langle J || \mu || J \rangle$$

Magnetic dipole operator: $$\boldsymbol{\mu} = \frac{e\hbar}{2m_p} \sum_i \left(g_i^l \boldsymbol{l}_i + g_i^s \boldsymbol{\sigma}_i \right)$$ Point-nucleon approximation

Neighbors of doubly magic: $$|J\rangle \approx |\mathrm{Core} : 0^+\rangle \otimes |j_p\rangle, \ j_p = J$$

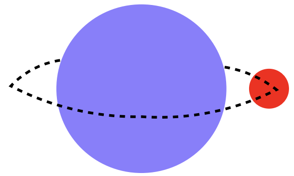

Schmidt limit

$$\langle \mu \rangle = \frac{e\hbar}{2m_p} \langle l_p j_p || g_i^l \boldsymbol{l}_i + g_i^s \boldsymbol{\sigma}_i || l_p j_p \rangle = j_p \left[g_l \mp (g_l - 2g_s) \frac{1}{2l_p + 1} \right], \ \left(j_p = l_p \pm \frac{1}{2} \right)$$

T. Schmidt 1937

Motivations

Configuration mixing effect: $$|J\rangle \approx c_0[|\mathrm{Core}:0^+\rangle \otimes |j_p\rangle] + \sum_i c_i[[|j_h^{-1}\rangle \otimes |j_q\rangle]_{J_i} \otimes |j_p\rangle]_J$$

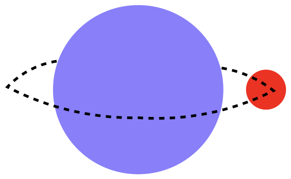

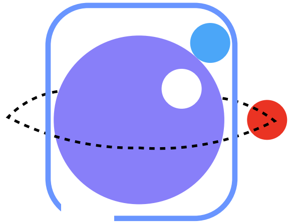

Core polarization

Arima and Horie computed c_i perturbatively: $$c \sim \frac{V}{\varepsilon}$$

NN interaction

SPE energy gap

A. Arima & H. Horie 1954

Good agreement with data.

- ✦ The deviation from the Schmidt value indicates how much the 0+ core is broken.

Motivations

Ab initio IMSRG calculations

✦ CP is included non-perturbatively!

A. Klose et al., Phys. Rev. C 99, 061301 (2019).

A			$Z = 20$		$N = 20$
	sp g^{free}	^{39}Ca	+1.148	^{39}K	+0.124
39	Expt.		+1.0217(1) [23]		+0.3915073(1) [24]
	sp g^{eff}		+0.930		+0.469
	VS-IMSRG		+1.349		−0.035
37	Expt.	^{37}Ca	+0.7453(72)	^{37}Cl	+0.6841236(4) [25]
	USDA-EM1		+0.770		+0.677
	USDB-EM1		+0.754		+0.675
	VS-IMSRG		+1.055		+0.290

of ^{36}Ca. Compared to the USDA/B-EM1 calculations, the VS-IMSRG agrees with the dominance of the (620) partition for ^{36}Ca. However, the amount of the (522) partition that gives the core-polarization correction is a factor of 2 larger. The deviation is likely due to meson-exchange currents [39], which are not included in the present VS-IMSRG calculations, but are included indirectly through the effective g factors in the USDA/B-EM1 calculations.

A. R. Vernon et al., Nature 607, 260 (2022).

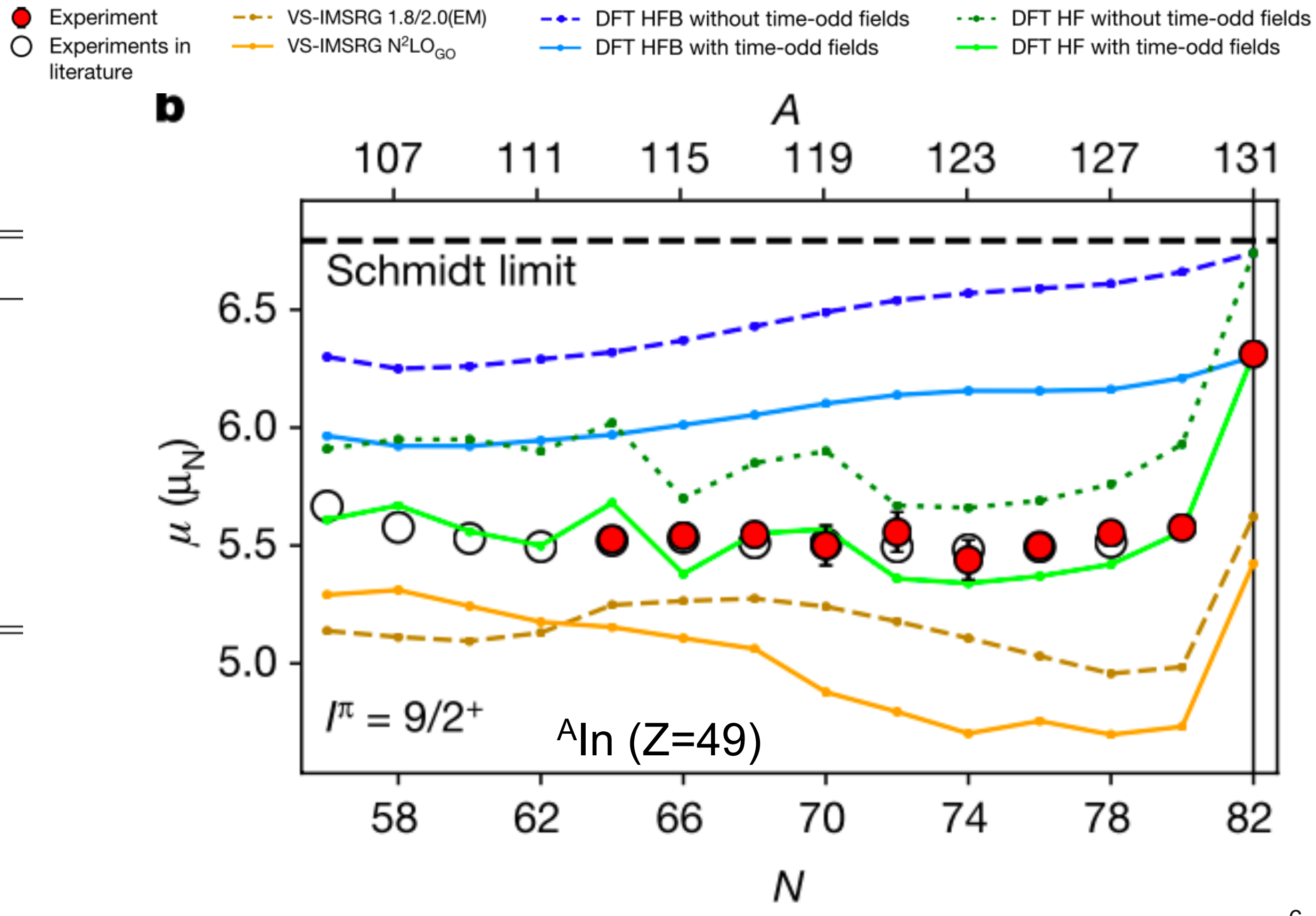

Nuclear ab initio calculation

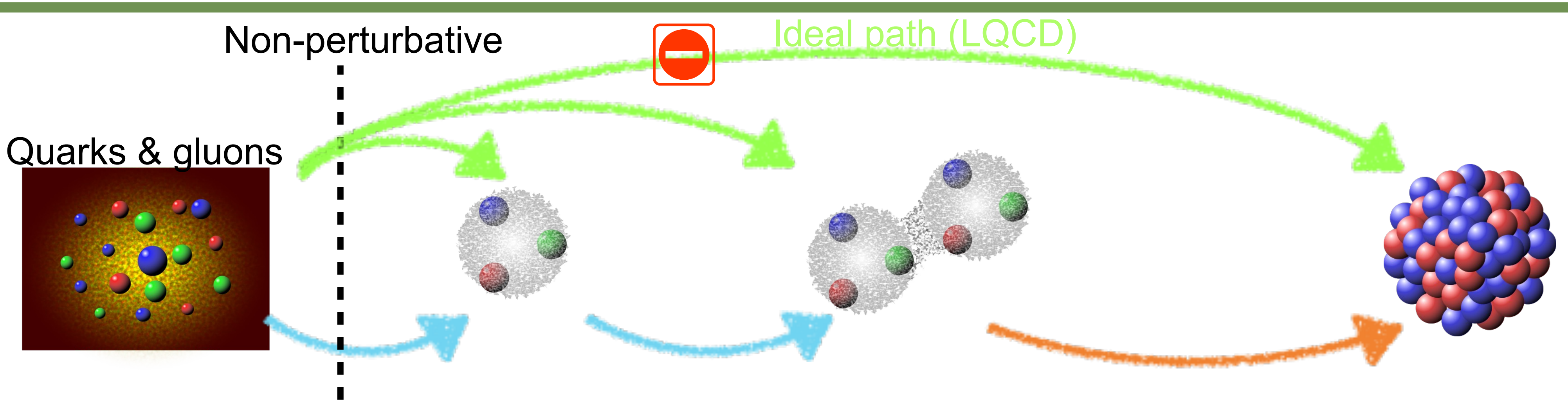

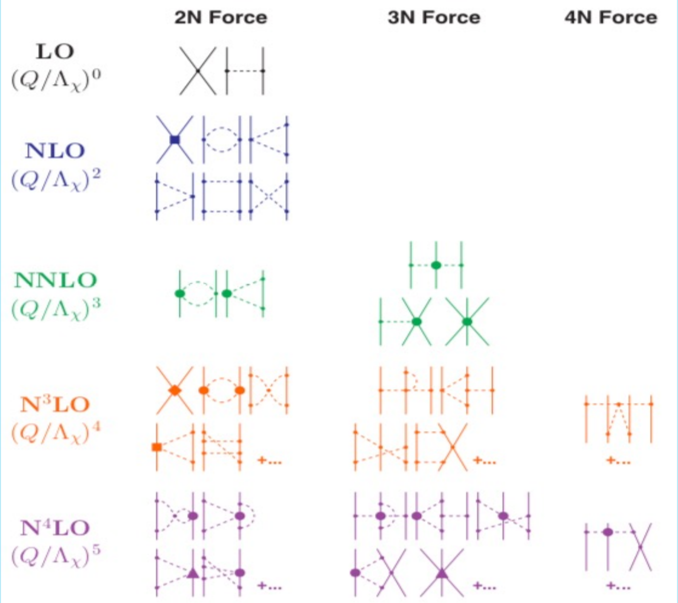

Nuclear many-body problem

- Green's function Monte Carlo
- No-core shell model
- Nuclear lattice effective field theory
- Self-consistent Green's function
- Coupled-cluster
- In-medium similarity renormalization group
- Many-body perturbation theory
- …

Nuclear interaction from chiral EFT

Weinberg, van Kolck, Kaiser, Epelbaum, Glöckle, Meißner, Entem, Machleidt, …

Lagrangian construction

- Chiral symmetry
- Power counting

Systematic expansion

- Unknown LECs
- Many-body interactions
- Estimation of truncation error

$Q = p/\Lambda$

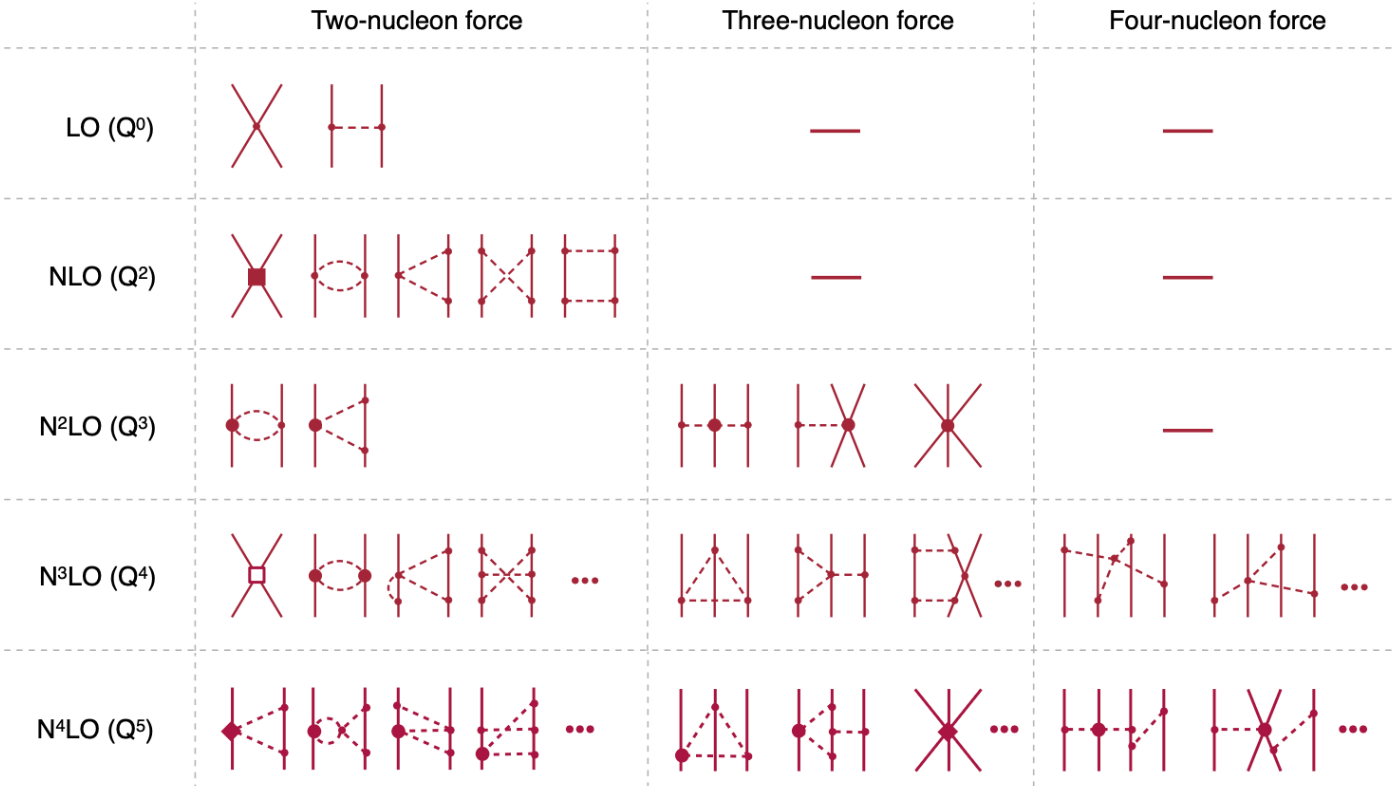

Figure is from E. Epelbaum, H. Krebs, and P. Reinert, Front. Phys. 8, 1 (2020).

Nuclear currents from chiral EFT

Nuclear observables (EM properties, beta decay, …) are measured through the interaction between a nucleus and external field.

Chiral EFT allows us a systematic expansion for charge and current operators.

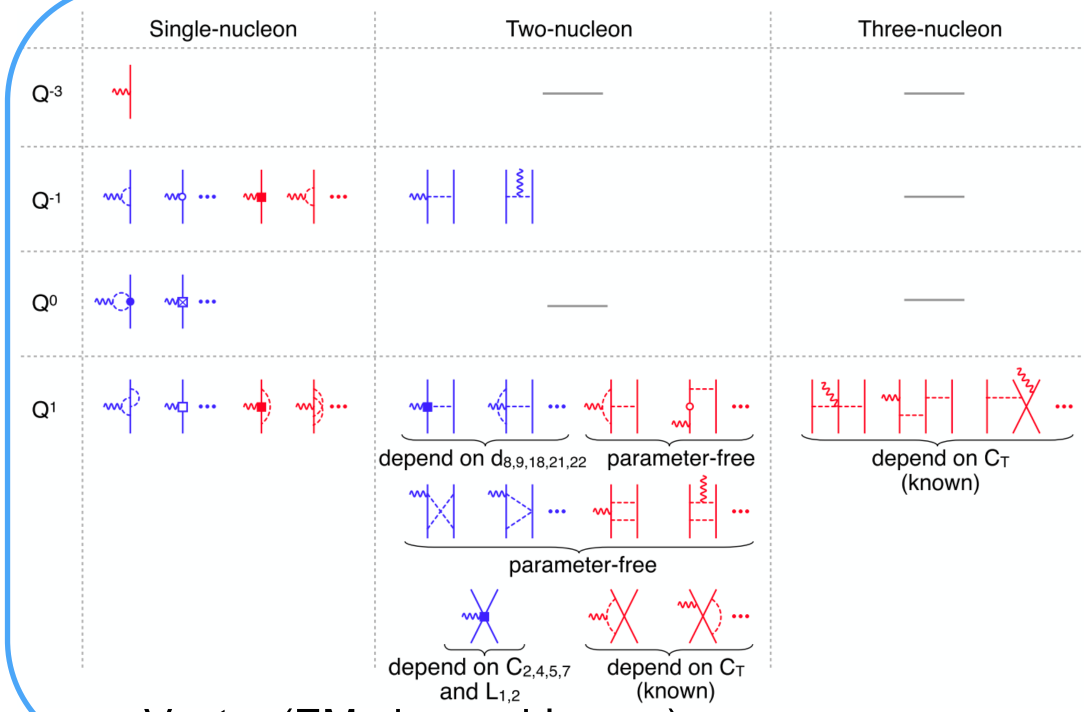

Vector (EM observables, …)

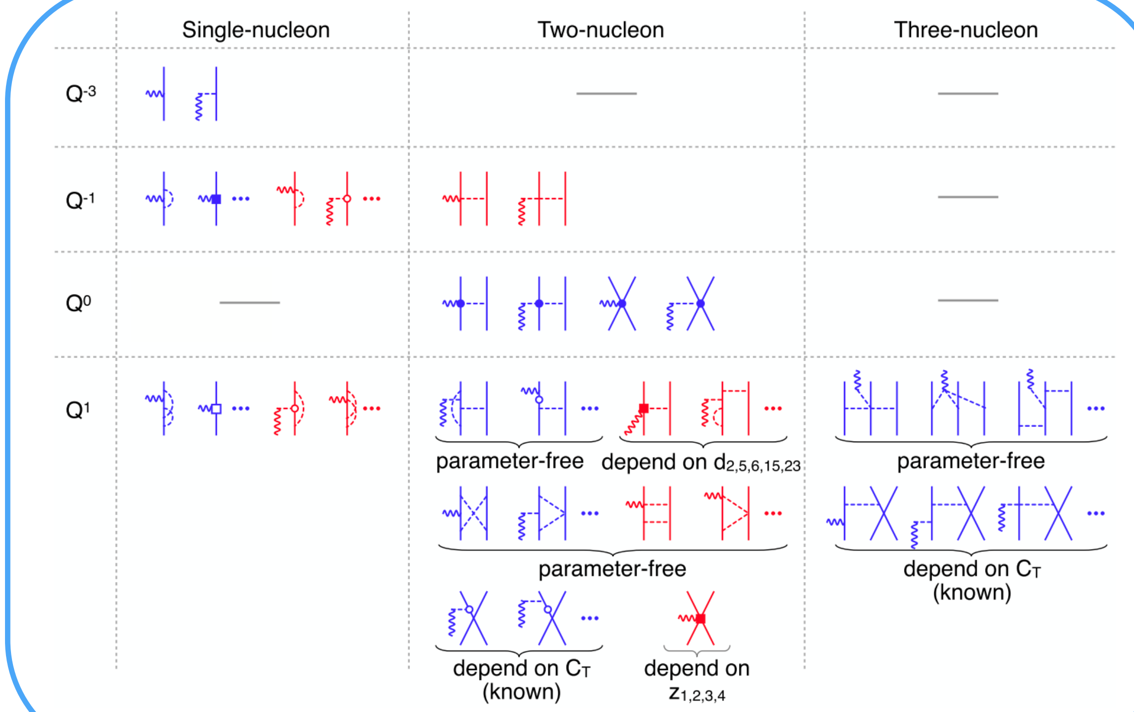

Axial vector (GT transition, …)

E. Epelbaum, arXiv:1908.09349.

Nuclear currents from chiral EFT

Nuclear observables (EM properties, beta decay, …) are measured through the interaction between a nucleus and external field.

Chiral EFT allows us a systematic expansion for charge and current operators.

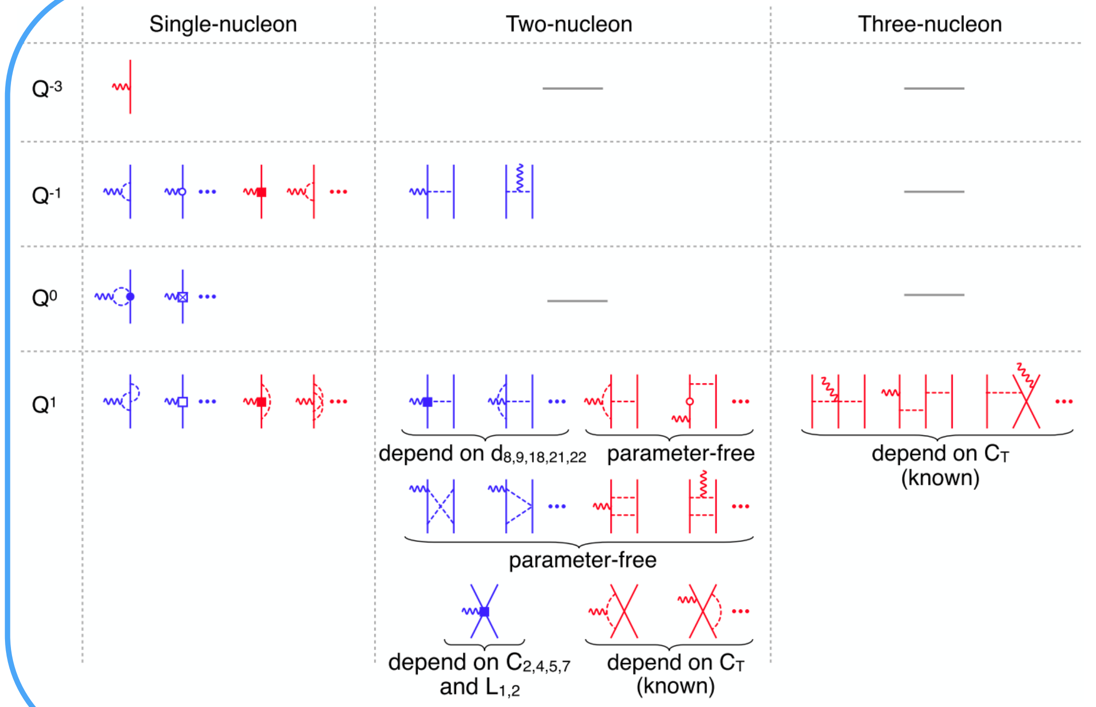

Vector (EM observables, …)

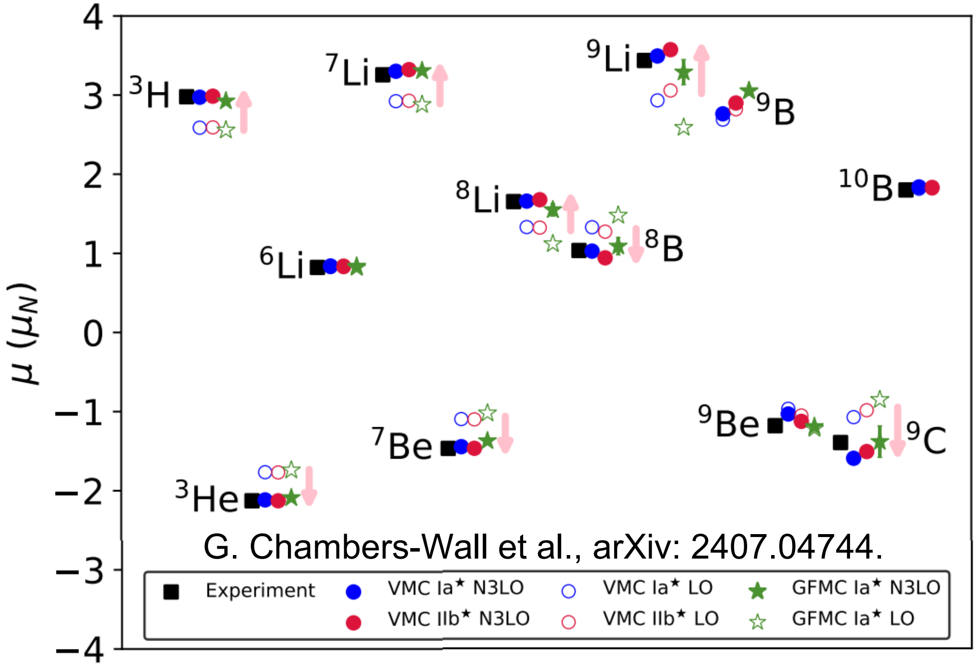

See talk by G. King for more details

What about in heavier systems?

Nuclear currents from chiral EFT

Nuclear observables (EM properties, beta decay, …) are measured through the interaction between a nucleus and external field.

Chiral EFT allows us a systematic expansion for charge and current operators.

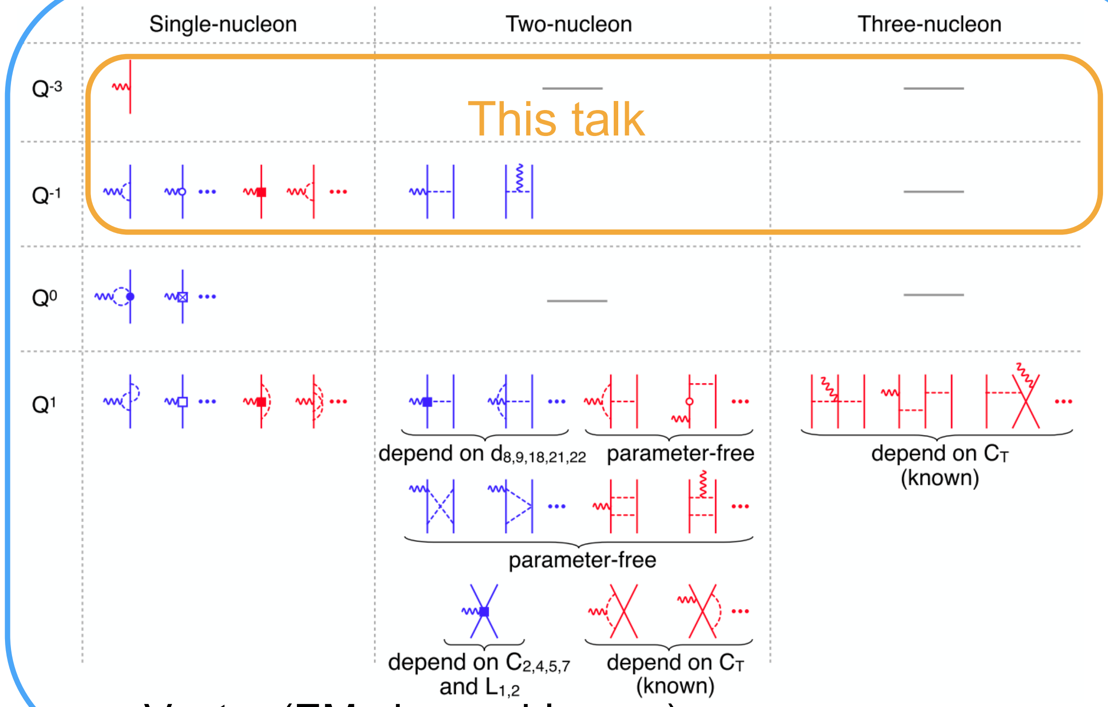

Vector (EM observables, …)

$$r_{ch}^2 = -\frac{6}{Z}\frac{1}{(4\pi)^{3/2}}\lim_{Q\to 0}\frac{d}{dQ^2}\int d\hat{\boldsymbol{Q}}\,\tilde{\rho}(\boldsymbol{Q})$$

LO 2BC appear at Q^1 order (N^3LO)

$$Q_{20} = -\frac{15}{8\pi}\lim_{Q\to 0}\frac{d^2}{dQ^2}\int d\hat{\boldsymbol{Q}}\,Y_{20}(\hat{\boldsymbol{Q}})\tilde{\rho}(\boldsymbol{Q})$$

$$M_{10} = -i\frac{3}{8\pi}\lim_{Q\to 0}\frac{d}{dQ}\int d\hat{\boldsymbol{Q}}\left\{[\boldsymbol{Q}\times\nabla_{\boldsymbol{Q}}]Y_{10}(\hat{\boldsymbol{Q}})\right\}\cdot\tilde{\boldsymbol{j}}(\boldsymbol{Q})$$

or $$\boldsymbol{M} = -\frac{i}{2}\sqrt{\frac{3}{4\pi}}\lim_{Q\to 0}\nabla_{\boldsymbol{Q}}\times\tilde{\boldsymbol{j}}(\boldsymbol{Q})$$

Valence-space in-medium similarity renormalization group

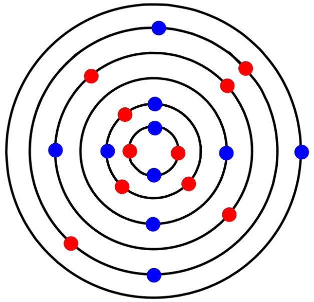

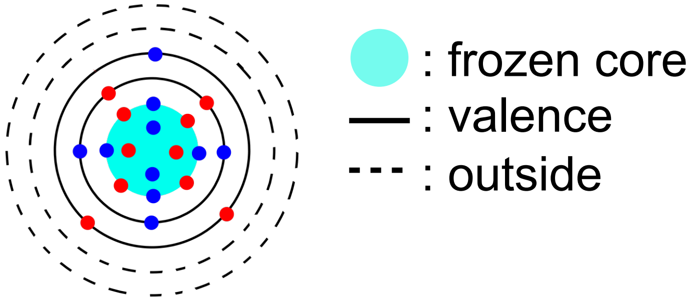

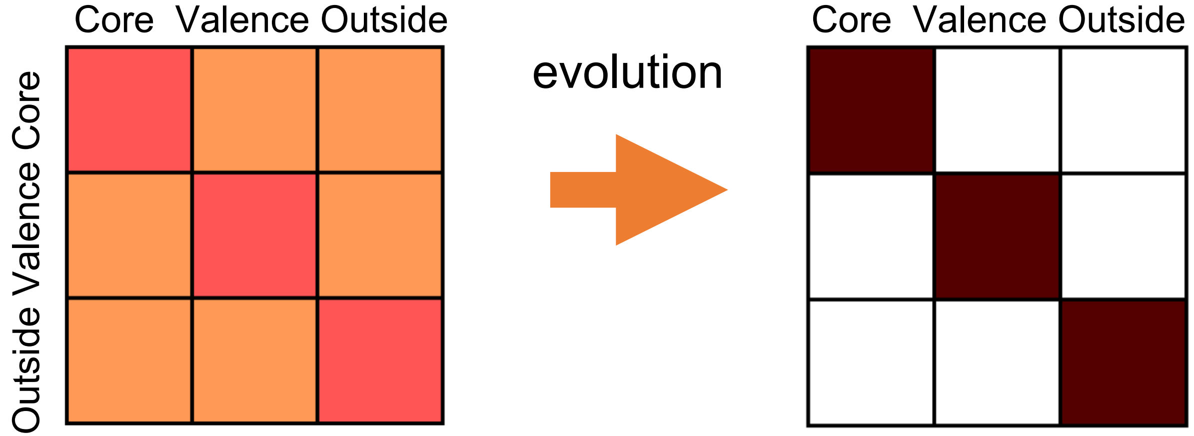

Similarity transformation

$$H \qquad\qquad H(s) = e^{\Omega(s)} H e^{-\Omega(s)}$$

$$H(s) \approx E(s) + \sum_{12} f_{12}(s)\{a_1^\dagger a_2\} + \frac{1}{4}\sum_{1234} \Gamma_{1234}(s)\{a_1^\dagger a_2^\dagger a_4 a_3\}$$

s: flow parameter

$$\frac{d\Omega}{ds} = \eta(s) - \frac{1}{2}[\Omega(s), \eta(s)] + \cdots$$

$$\eta(s) = \sum_{12} \eta_{12}(s)\{a_1^\dagger a_2\} + \sum_{1234} \eta_{1234}(s)\{a_1^\dagger a_2^\dagger a_4 a_3\}$$

$$\eta_{12} = \frac{1}{2}\arctan\left(\frac{2f_{12}}{f_{11} - f_{22} + \Gamma_{1212} + \Delta}\right)$$

$$\eta_{1234} = \frac{1}{2}\arctan\left(\frac{2\Gamma_{1234}}{f_{11} + f_{22} - f_{33} - f_{44} + A_{1234} + \Delta}\right)$$

$$A_{1234} = \Gamma_{1212} + \Gamma_{3434} - \Gamma_{1313} - \Gamma_{2424} - \Gamma_{1414} - \Gamma_{2323}$$

f_{12}, Γ_{1234} : matrix element we want to suppress

$$\mathcal{O}(s) = e^{\Omega(s)} \mathcal{O} e^{-\Omega(s)} \approx \mathcal{O}^{[0]}(s) + \sum_{12} \mathcal{O}^{[1]}_{12}(s)\{a_1^\dagger a_2\} + \frac{1}{4}\sum_{1234} \mathcal{O}^{[2]}_{1234}(s)\{a_1^\dagger a_2^\dagger a_4 a_3\}$$

Valence-space in-medium similarity renormalization group

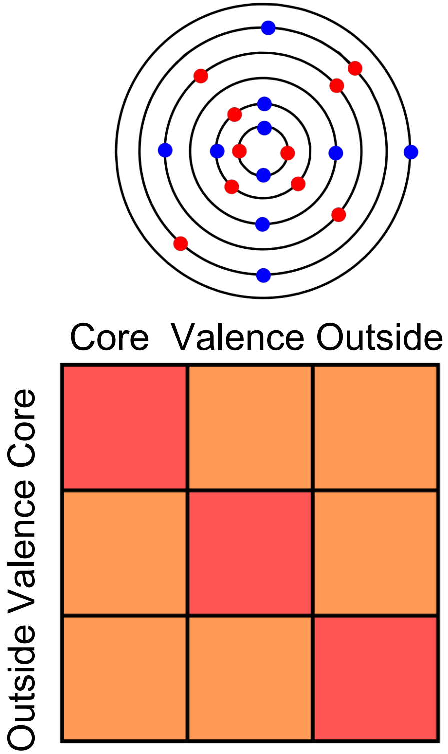

evolution

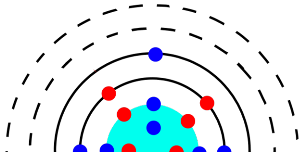

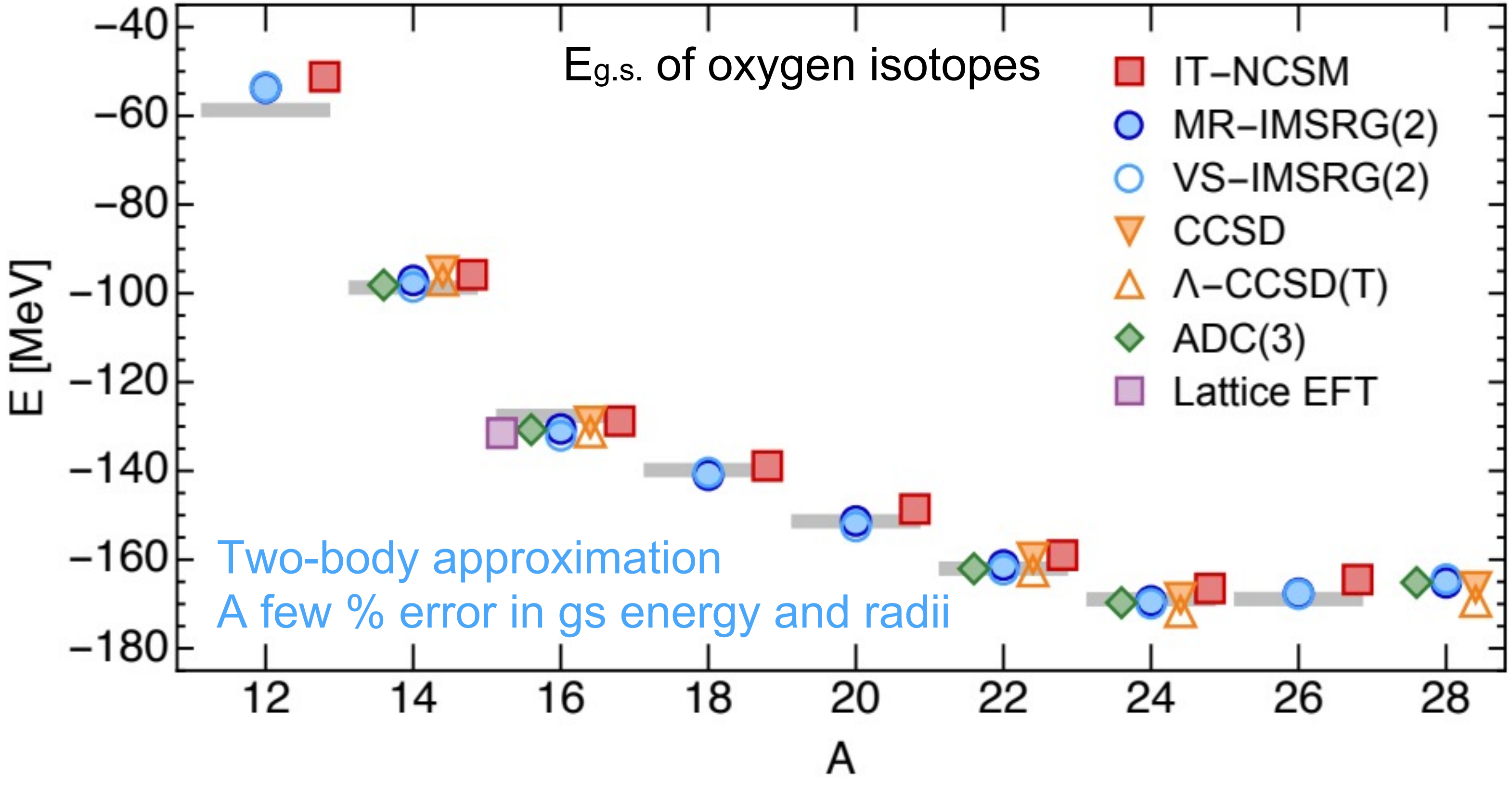

Similarity transformat

H

$$H(s) \approx E(s) + \sum_{12} f_{12}(s)\{a_1^\dagger a_2\} + \frac{1}{4} \quad {}_{1234}$$

s: flow parameter

Magnetic dipole moments

Magnetic moment from IMSRG.

- 1.8/2.0 (EM) interaction (see talk by P. Arthuis)

Single-particle analytical limits do not always explain the experimental data.

A better agreements with IMSRG, but not perfect.

- Suppression from many-body correlation

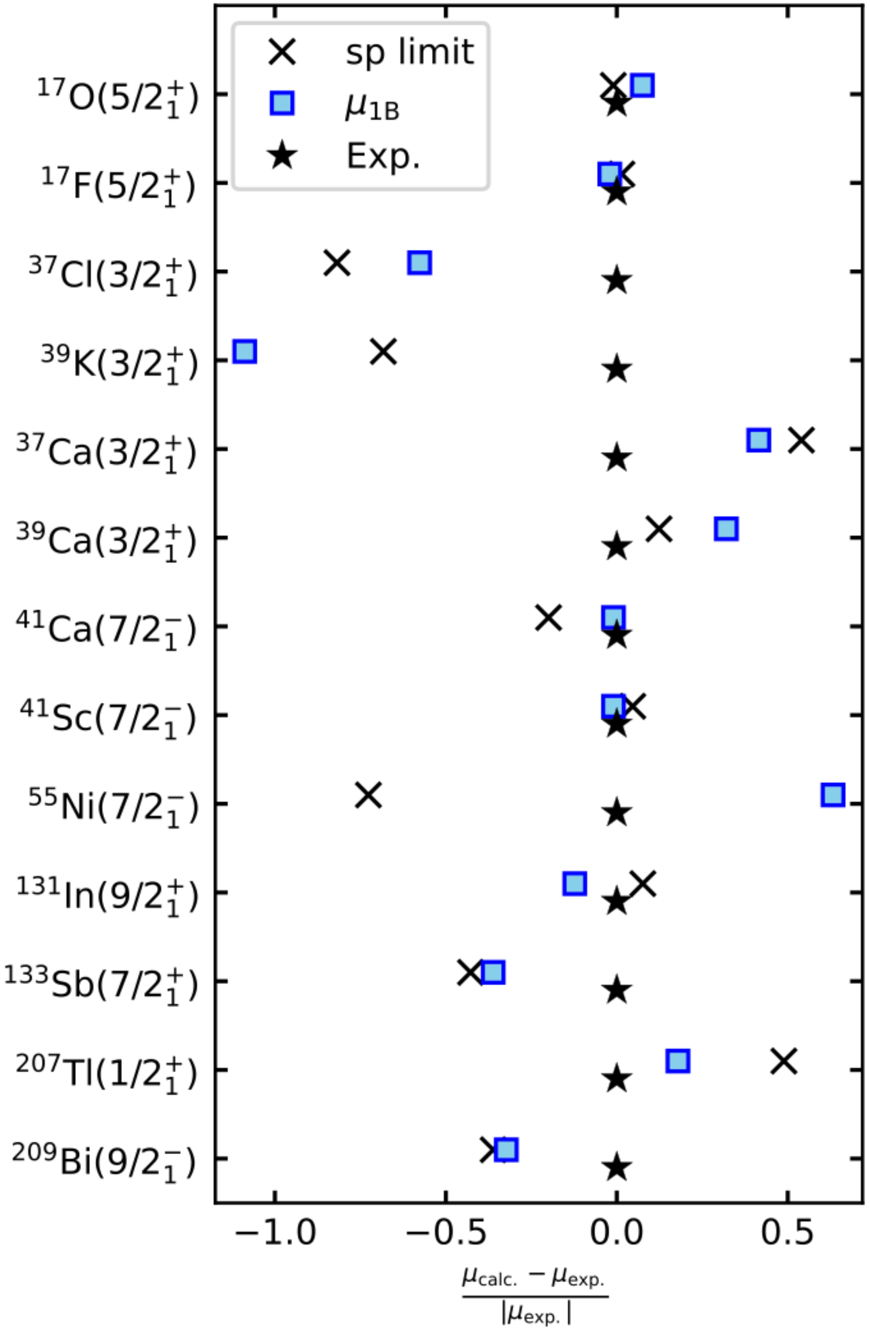

TM et al., Phys. Rev. Lett. **132**, 232503 (2024).

Magnetic dipole moments

Magnetic moment from IMSRG.

- 1.8/2.0 (EM) interaction (see talk by P. Arthuis)

Single-particle analytical limits do not always explain the experimental data.

A better agreements with IMSRG, but not perfect.

2BC globally improves the magnetic moments.

- Enhancement from 2BC

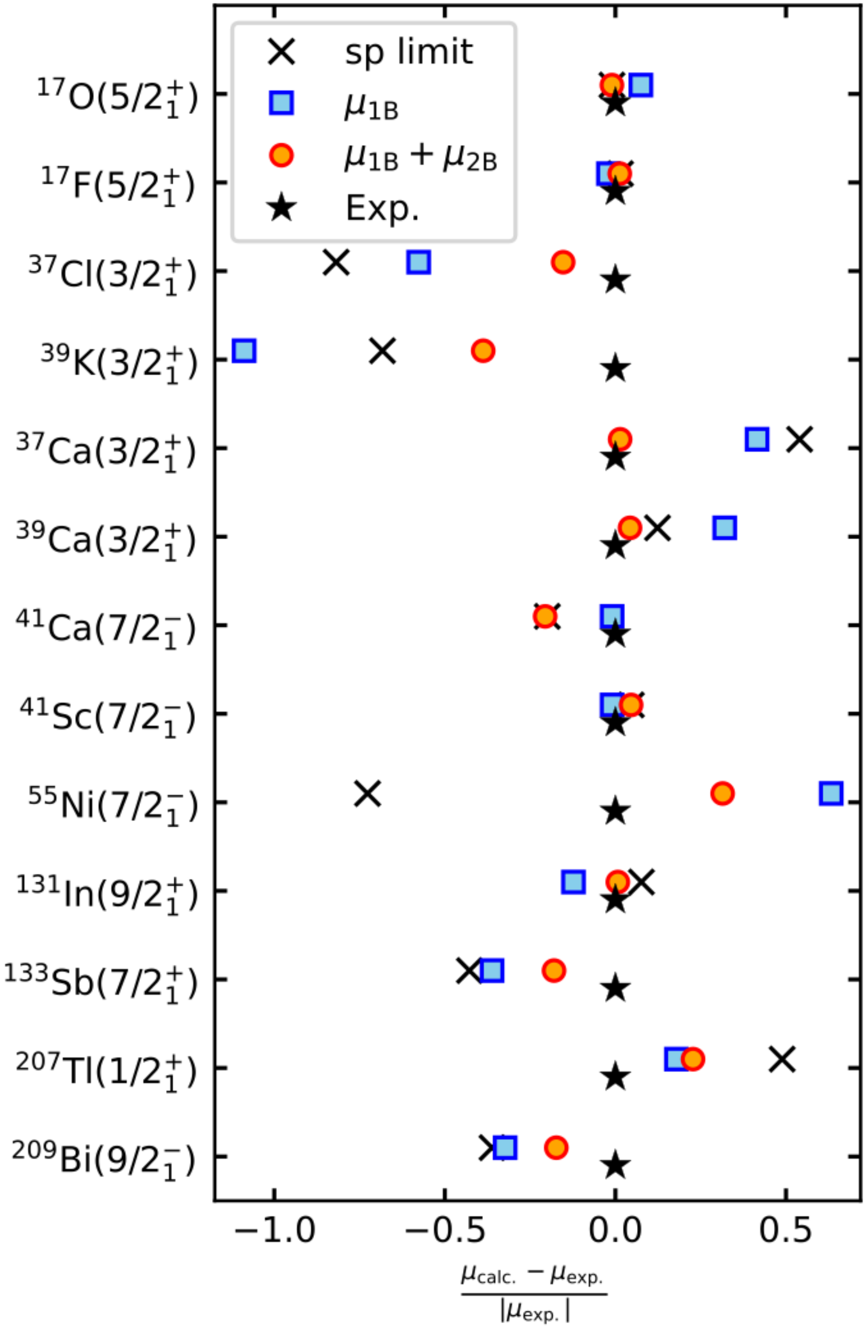

TM et al., Phys. Rev. Lett. **132**, 232503 (2024).

4th moment of charge density

筑波大学 計算科学研究センター Center for Computational Sciences

Recent precise mass and laser spectroscopy measurements —> new physics

$$\nu^A - \nu^{A'} = K\mu_{A,A'} + F\delta\langle r^2\rangle_{A,A'} + G^{(2)}[\delta\langle r^2\rangle^2]_{A,A'} + G^{(4)}\delta\langle r^4\rangle_{A,A'} + \cdots + (\text{new physics})$$

M. Door et al., arXiv:2403.07792

Combination with the MCSM technique was essential.

N. Shimizu et al., Phys. Rev. C 103, 014312 (2021).
See talk by T. Otsuka

Precise atomic and nuclear theories are needed.

- Extracted delta<r^4>
  - Hamiltonian uncertainty sizable
  - Valence-space uncertainty small
  - Small many-body uncertainty was estimated
  - Flat trend over the isotopes

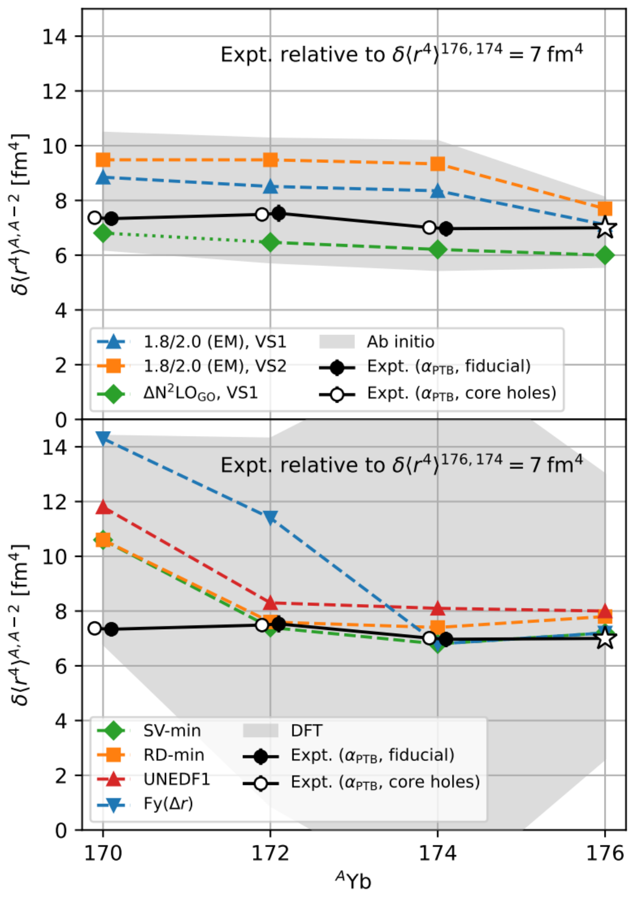

4th moment of charge density

筑波大学 計算科学研究センター Center for Computational Sciences

In M. Door et al., arXiv:2403.07792, only the R_p^4 was computed.

4th moment of charge density: $$R_{\rm ch}^4 = \frac{60}{F_{\rm ch}(0)} \lim_{q\to 0} \frac{d}{dq^2}\frac{d}{dq^2} F_{\rm ch}(q).$$

Charge form factor: $$F_{\rm ch}(q) = e\sum_{i=1}^{A}\left\{G_i^E(q^2)\left[1-\frac{q^2}{8m^2}\right] j_0(x_i) - \frac{q^2}{2m^2}\left[G_i^M(q^2)-\frac{1}{2}G_i^E(q^2)\right](\boldsymbol{\ell}_i\cdot\boldsymbol{\sigma}_i)\frac{j_1(x_i)}{x_i}\right\},$$

$x_i = q|\boldsymbol{r}_i - \boldsymbol{R}_{\rm cm}|$ G^E and G^M are Sachs form factors

R_{ch}^4: $$R_{\rm ch}^4 = R_p^4 + \frac{10}{3}\left(r_p^2 R_p^2 + \frac{N}{Z} r_n^2 R_n^2\right) + \frac{5}{2m^2}\left(R_p^2 + r_p^2 + \frac{N}{Z} r_n^2\right) + r_p^4 + \frac{N}{Z} r_n^4 + R_{\rm SO}^4$$

See also:
H. Kurasawa and T. Suzuki, Prog. Theor. Exp. Phys., 113D01 (2019).
H. Kurasawa and T. Suzuki, Prog. Theor. Exp. Phys., 013D02 (2020).
T. Suzuki, R. Danjo, T. Suda, Prog. Theor. Exp. Phys., 093D02 (2024).

4th moment of charge density

筑波大学 計算科学研究センター Center for Computational Sciences

The Rch4 operator looks like the 4-body operator —> $R^4_{\rm ch} = \frac{60}{F_{\rm ch}(0)} \lim_{q\to 0} \frac{d}{dq^2}\frac{d}{dq^2} F_{\rm ch}(q).$

Gaussian process:

- Derivative is also a Gaussian process

^{3}H, Jacobi NCSM, 1.8/2.0 (EM)

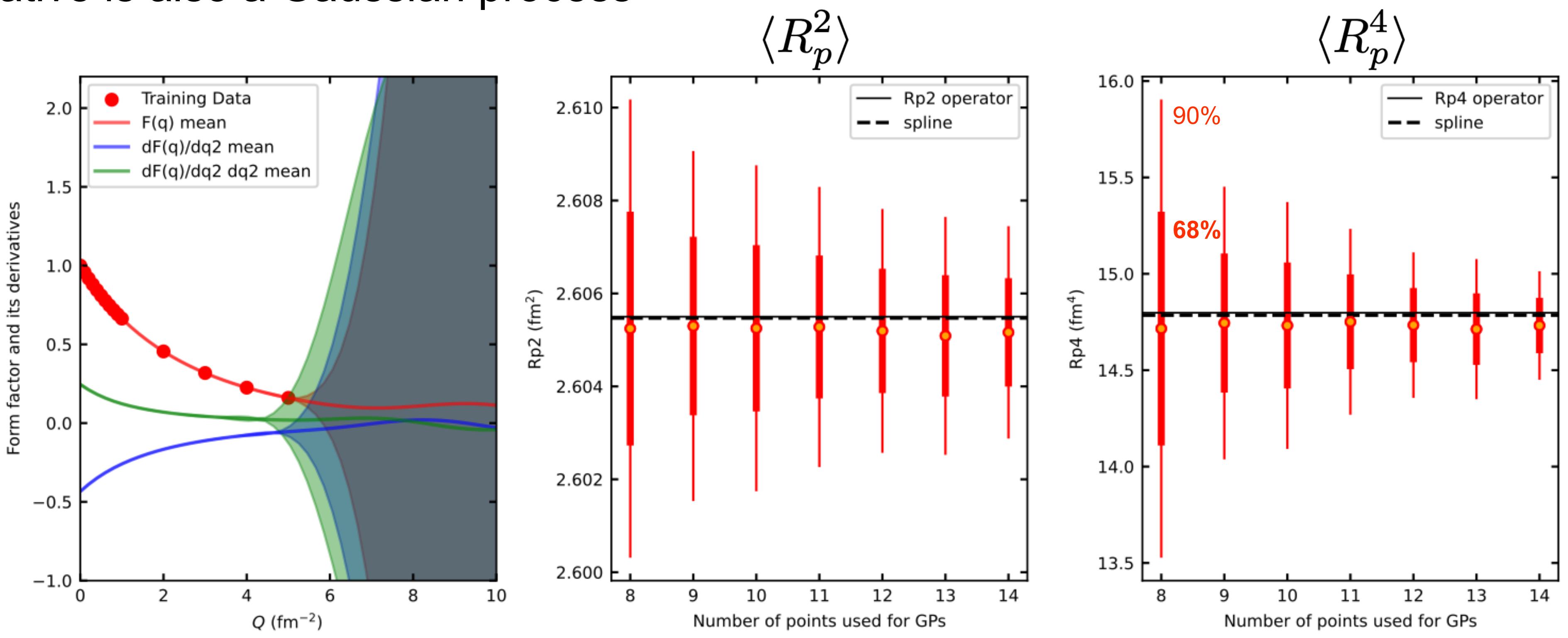

4th moment of charge density

Correlations

^{208}Pb with 34 non-implausible interactions [*B. S. Hu et al., Nat. Phys. 18, 1196 (2022).]
Sachs form factors: Z. Ye, J. Arrington, R. J. Hill, and G. Lee, Phys. Lett. B 777, 8 (2018)

$$r_{XY} = \frac{\mathrm{Cov}[X, Y]}{\sigma_X \sigma_Y}$$

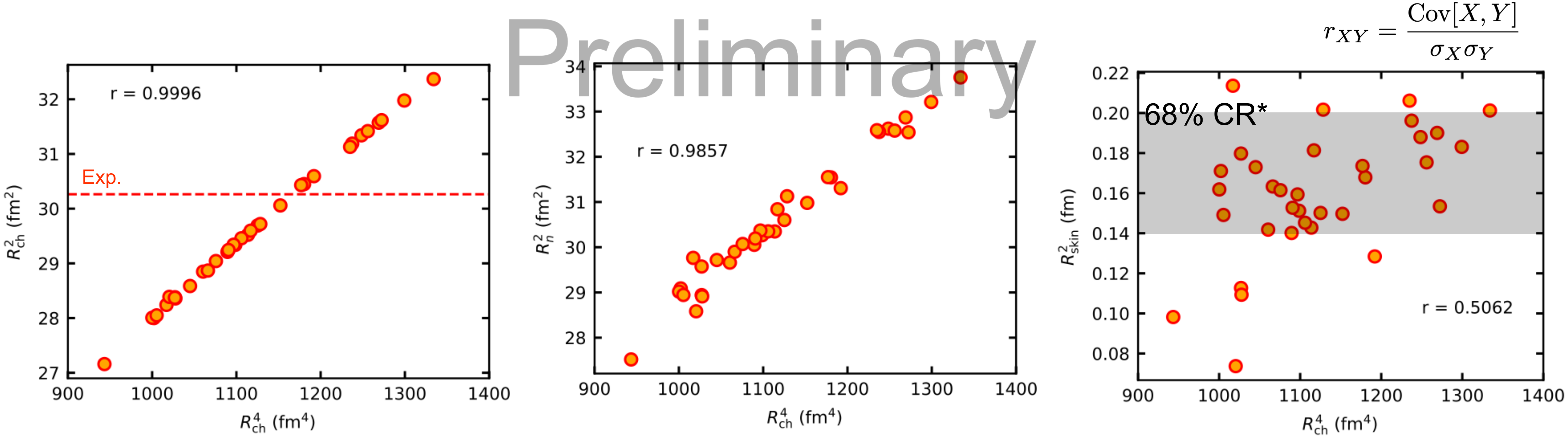

The correlation is strong for Rch2 and Rn2, while it is weak for Rskin

Uncertainty quantification is not completed yet.

Summary

Magnetic dipole moments

- For most of doubly-closed shell nuclei +/- 1 systems, the 2BC improves the agreements.

4th moment of charge density of ^{208}Pb

- Strong correlation with ms charge and neutron radii

Future works:

- 2BC effect with finite momentum transfer Q
- Exploring how we can leverage the correlation of R_{ch}^4 and the other observables.
- Uncertainty quantification

Backup slides

Normal ordering wrt a single Slater determinant

Initial Hamiltonian is expressed with respect to nucleon vacuum

$$H = \sum_{pq} t_{pq} a_p^\dagger a_q + \frac{1}{4} \sum_{pqrs} V_{pqrs} a_p^\dagger a_q^\dagger a_s a_r + \frac{1}{36} V_{pqrstu} a_p^\dagger a_q^\dagger a_r^\dagger a_u a_t a_s$$

- Hamiltonian normal ordered with respect to a single Slater determinant

$$H = E_0 + \sum_{pq} f_{pq} \{a_p^\dagger a_q\} + \frac{1}{4} \sum_{pqrs} \Gamma_{pqrs} \{a_p^\dagger a_q^\dagger a_s a_r\} + \frac{1}{36} W_{pqrstu} \{a_p^\dagger a_q^\dagger a_r^\dagger a_u a_t a_s\}$$

$$E_0 = \sum_{pq} t_{pq} \rho_{pq} + \frac{1}{2} \sum_{pqrs} V_{pqrs} \rho_{pr} \rho_{qs} + \frac{1}{6} \sum_{pqrstu} V_{pqrstu} \rho_{ps} \rho_{qt} \rho_{ru}, \qquad \Gamma_{pqrs} = V_{pqrs} + \sum_{tu} V_{pqtrsu} \rho_{tu}$$

$$f_{pq} = t_{pq} + \sum_{rs} V_{prqs} \rho_{rs} + \frac{1}{2} \sum_{rstu} V_{prsqtu} \rho_{rt} \rho_{su}, \qquad W_{pqrstu} = V_{pqrstu}$$

- Normal ordered two-body (NO2B) approximation:

$$H \approx E_0 + \sum_{pq} f_{pq} \{a_p^\dagger a_q\} + \frac{1}{4} \sum_{pqrs} \Gamma_{pqrs} \{a_p^\dagger a_q^\dagger a_s a_r\}$$

Model-space convergence

NN+3N Hamiltonian (harmonic oscillator basis)

Parameters:

- hw
- e_{max}=max(2n+l)*
- E_{3max}=max(e_1+e_2+e_3).

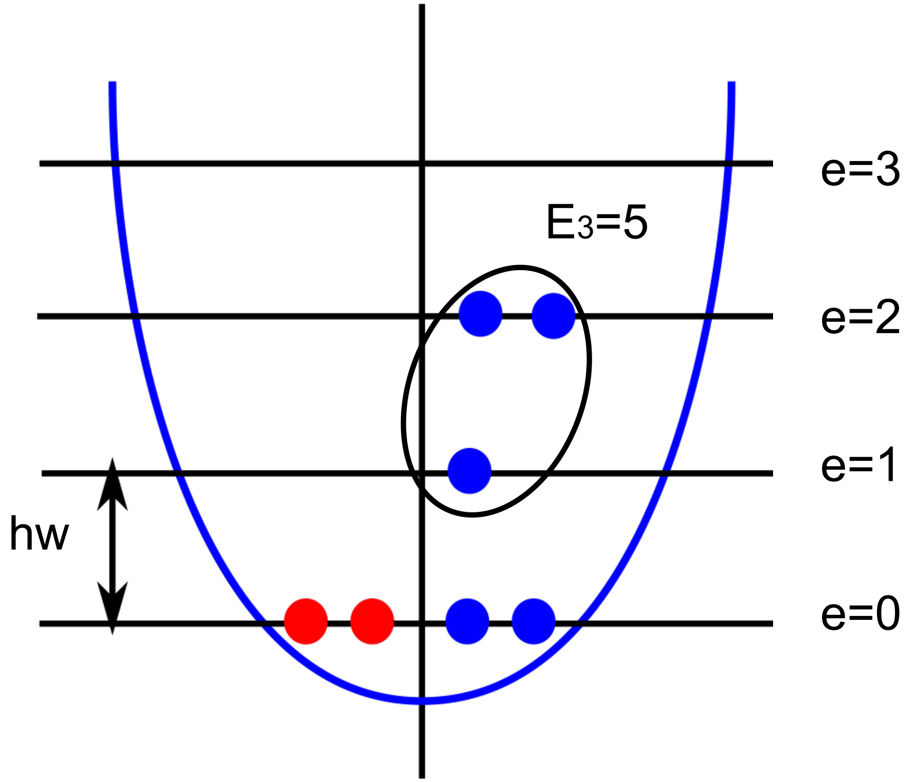

As e_{max} and E_{3max} increases, the observable should not depend on all the parameters.

*Equivalent to (number of major shells)+1

$E_{3\max}$ convergence in heavy nuclei

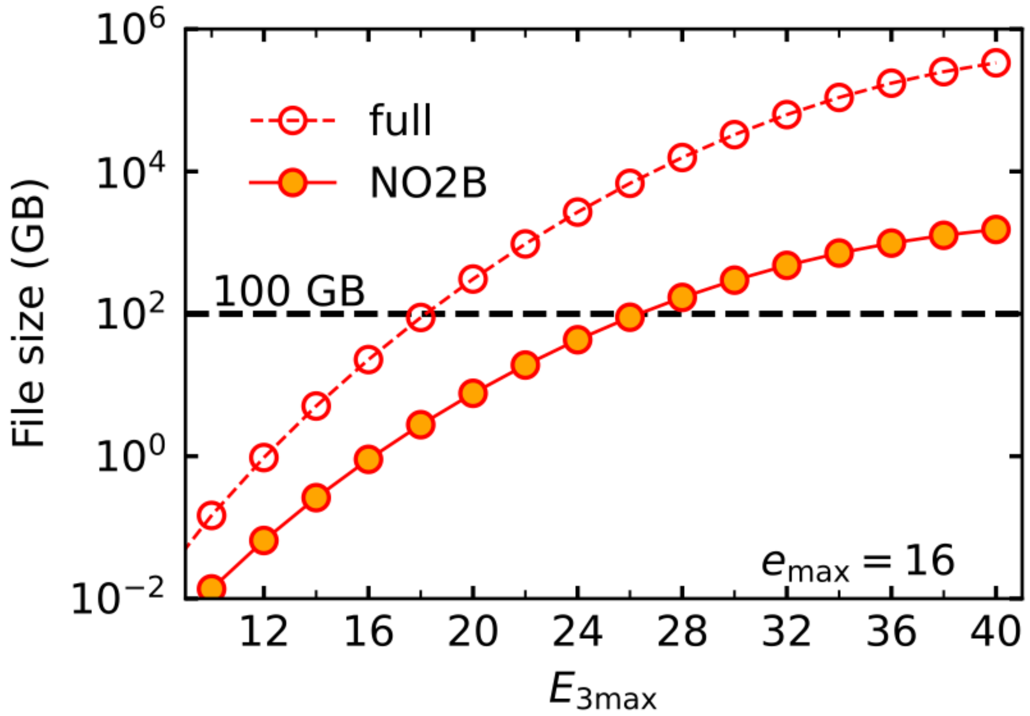

TM, S. R. Stroberg, P. Navrátil, K. Hebeler, and J. D. Holt, Phys. Rev. C 105, 014302 (2022).

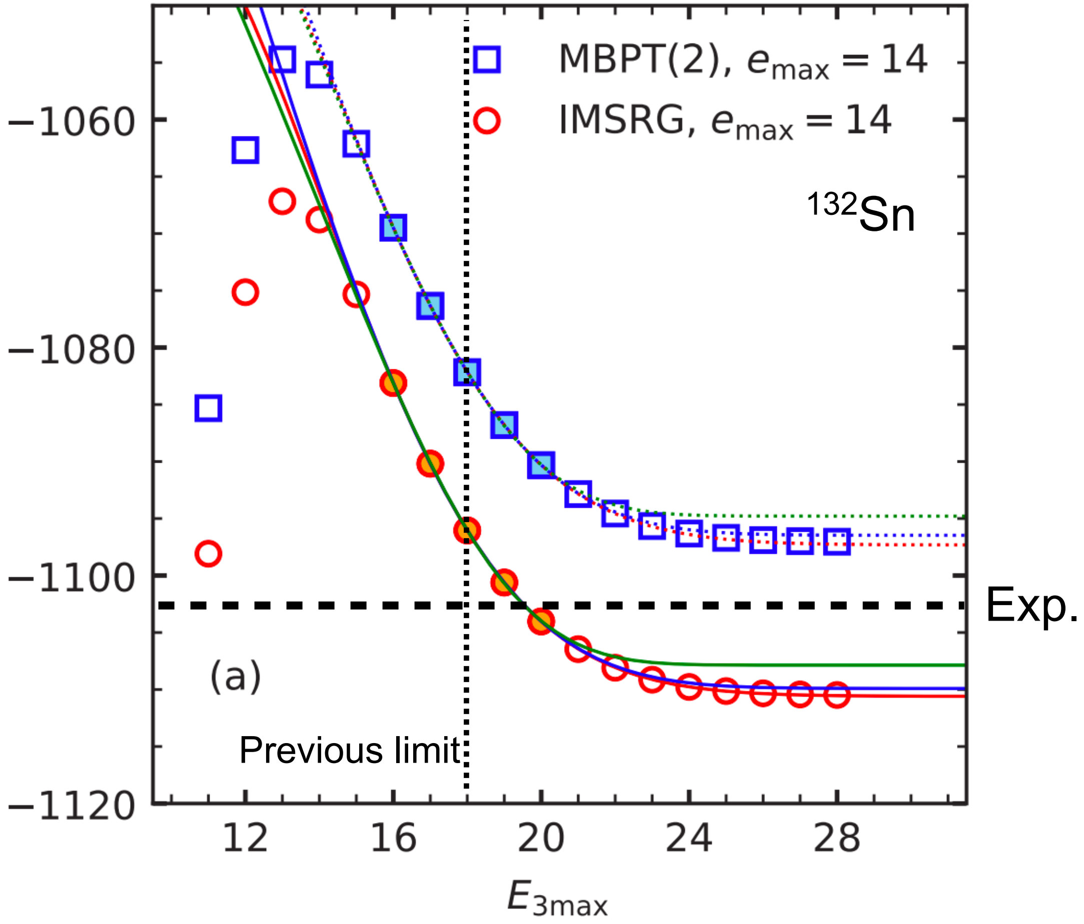

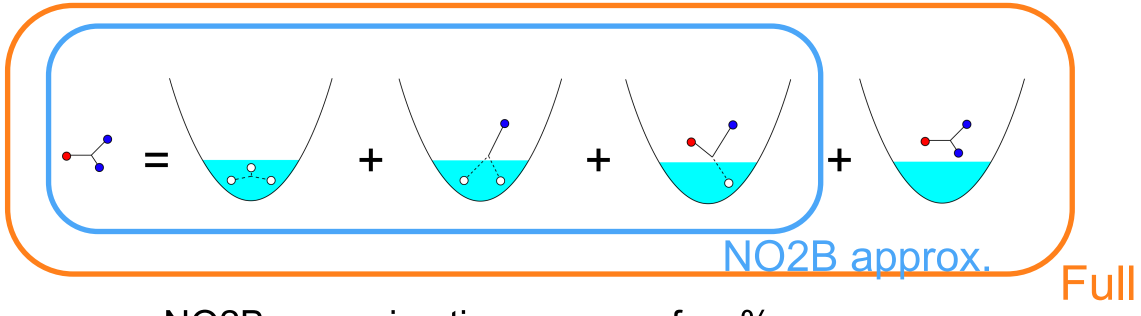

NO2B approximation error ~ a few %
[S. Binder et al., Phys. Rev. C 87, 021303 (2013).]

Asymptotic form: $E \approx A\gamma_{\frac{2}{n}}\left[\left(\frac{E_{3\max}-\mu}{\sigma}\right)^{n}\right] + E_{\infty}$

Radii

TM, S. R. Stroberg, P. Navrátil, K. Hebeler, and J. D. Holt, Phys. Rev. C 105, 014302 (2022).

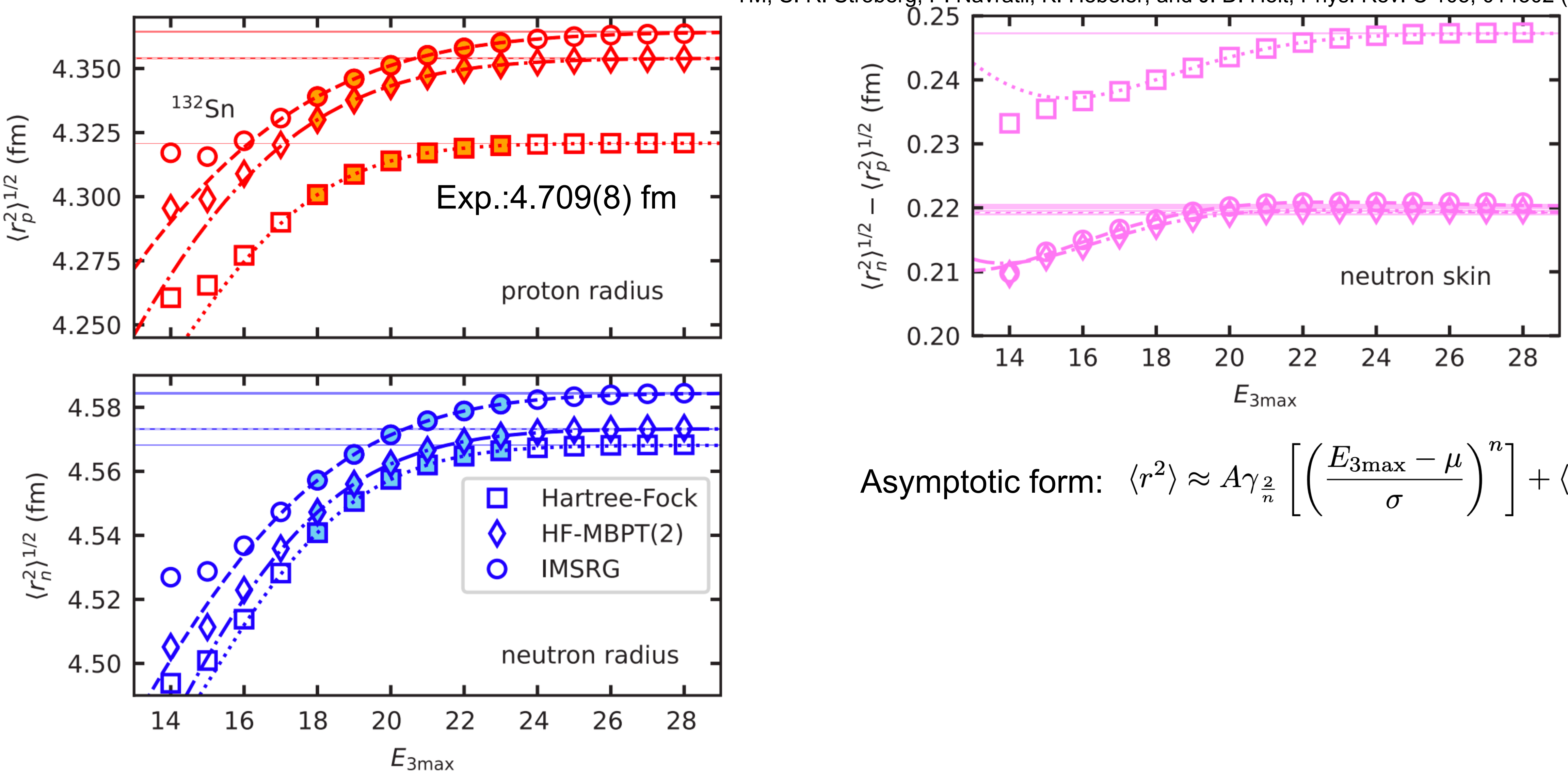

Asymptotic form: $\langle r^2\rangle \approx A\gamma_{\frac{2}{n}}\left[\left(\frac{E_{3\max}-\mu}{\sigma}\right)^n\right] + \langle r^2\rangle_\infty$

Convergence of ^{209}Bi

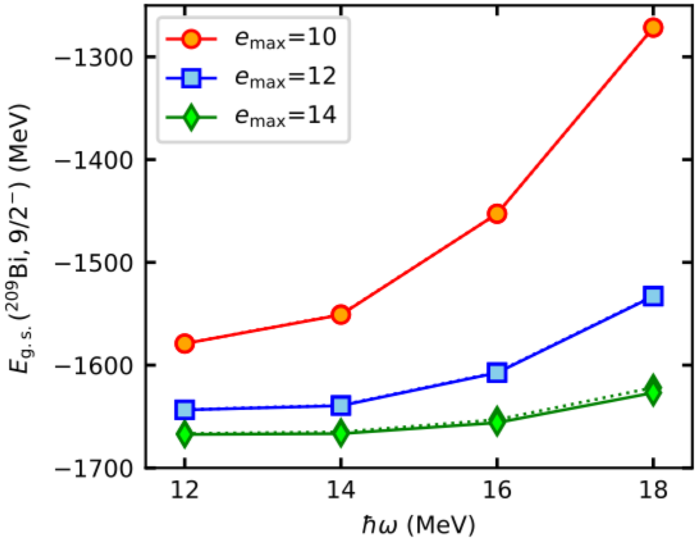

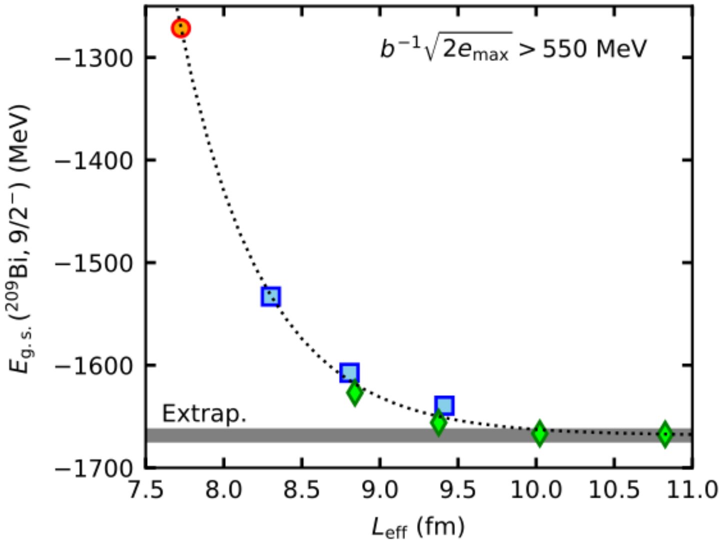

$$E(L_{\text{eff}}) = E_\infty + A_\infty \exp(-2k_\infty L_{\text{eff}})$$

$$L_{\text{eff}} = \sqrt{\frac{\sum_{nl} n_{nl}^{\text{occ}} a_{nl}^2}{\sum_{nl} n_{nl}^{\text{occ}} \kappa_{nl}^2}}, \quad \kappa_{nl}^2 \approx \frac{a_{nl}^2}{2b^2(N_l + 7/2)}$$

$$b^2 = \frac{\hbar}{m\omega}$$

$$N_l = \begin{cases} e_{\max} & e_{\max} + l \equiv 0 \pmod 2 \\ e_{\max} - 1 & e_{\max} + l \equiv 1 \pmod 2 \end{cases}$$

n_{nl}^{occ} : occupation number of an orbit specified by n and l

a_{nl} : $(n+1)$-th zero of the spherical Bessel function

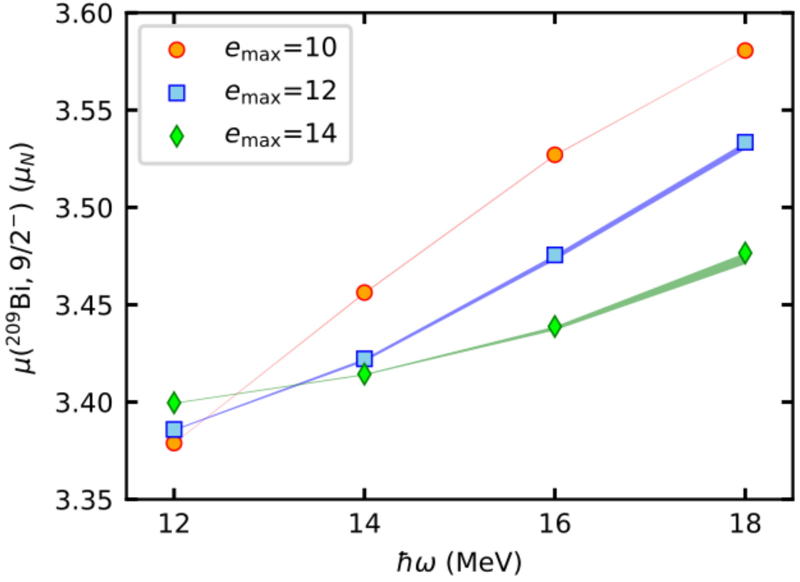

Magnetic moments of In isotopes

筑波大学
計算科学研究センター
Center for Computational Sciences

VS-IMSRG(2), 1.8/2.0 (EM), e_{max}=14, E_{3max}=24, hw = 16 MeV

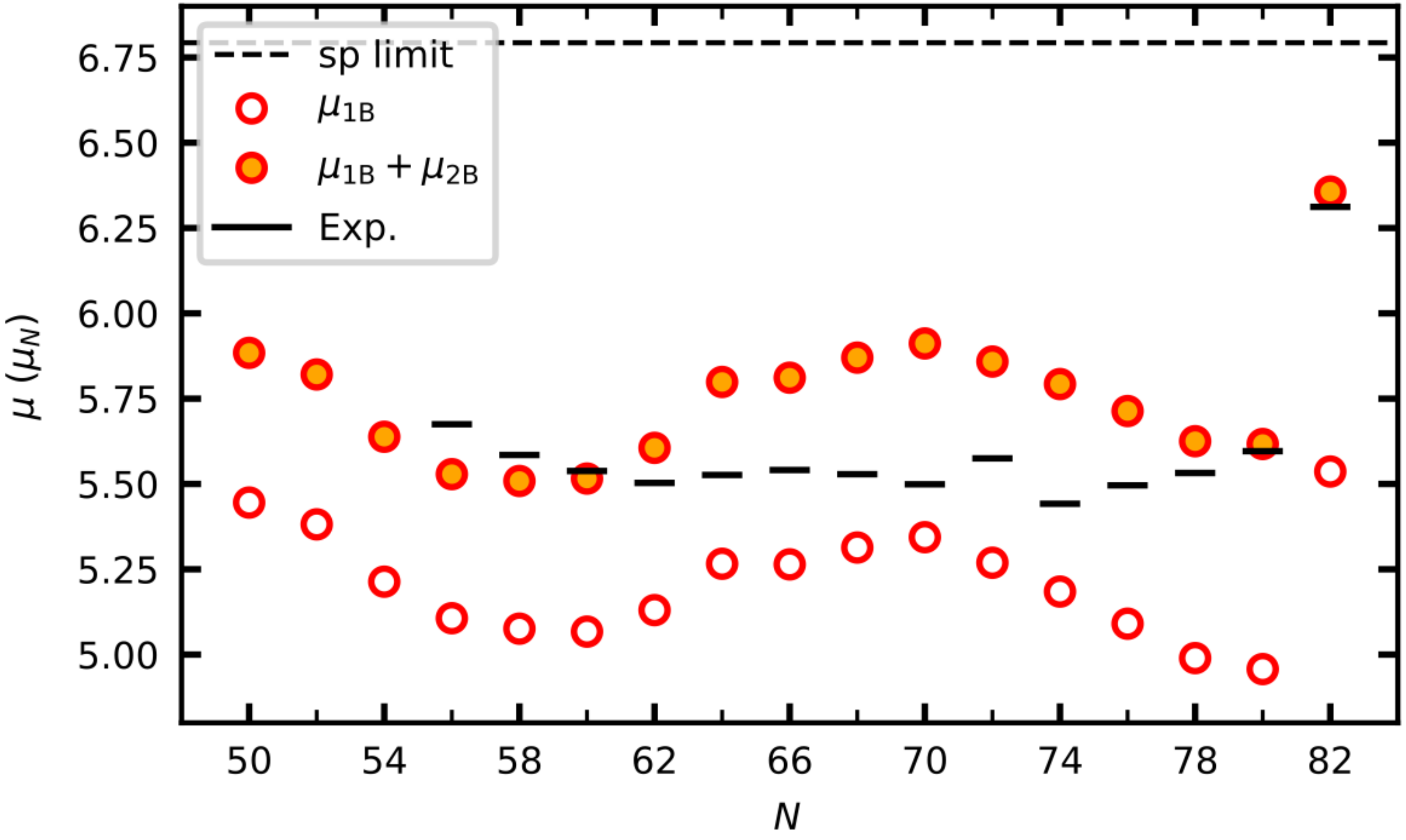

2B contribution with the simplest limit

Expectation value: $\langle J||\mu||J\rangle$

The simplest limit: $|JM\rangle = [|j_1 \dots j_{A-1} : 0^+\rangle \otimes |j_p m_p\rangle]\delta_{j_p J}\delta_{m_p M}$

The expectation value depends a particle in the core and last unpaired particle.

$$
\begin{aligned}
\langle J||\mu||J\rangle &\approx \delta_{Jj_p} \sum_{q\in\mathrm{core}} \langle p0 : j_p||\mu_{pq}||p0 : j_p\rangle \\
&= \delta_{Jj_p} \sum_{q\in\mathrm{core}} \sum_{I} \frac{2I+1}{(2j_p+1)(2j_q+1)} \langle ((pq)I, q : j_p||\mu_{pq}||(pq)I, q : j_p\rangle \\
&= \delta_{Jj_p} \sum_{q\in\mathrm{core}} \sum_{I} \frac{2I+1}{2j_q+1} (-1)^{j_p+j_q+I+1} \left\{ \begin{array}{ccc} j_p & I & j_q \\ I & j_p & 1 \end{array} \right\} \langle pq : I||\mu||pq : I\rangle
\end{aligned}
$$

2B contribution with the simplest limit

筑波大学 計算科学研究センター Center for Computational Sciences

The simplest limit: $|JM\rangle = [|j_1 \dots j_{A-1} : 0^+\rangle \otimes |j_p m_p\rangle]\delta_{j_p J}\delta_{m_p M}$

A simpler expression:

$$\langle \mu \rangle \sim \sum_{q \in \mathrm{core}} \langle pq|\bar{\mu}|pq\rangle$$

$$\langle pq|\bar{\mu}|pq\rangle = \delta_{Jj_p}\sqrt{\frac{1}{2J+1}}\mathcal{C}^{J1J}_{J0J}\sum_I \frac{2I+1}{2j_q+1}(-1)^{j_p+j_q+I+1}\left\{\begin{array}{ccc} j_p & I & j_q \\ I & j_p & 1 \end{array}\right\}$$

$$\times \frac{\sqrt{2I+1}}{\mathcal{C}^{I1I}_{J+m_q 0 J+m_q}}\left[\mathcal{C}^{j_p j_q I}_{J m_q J+m_q}\right]^2 \frac{1}{1+\delta_{n_p n_q}\delta_{l_p l_q}\delta_{j_p j_q}\delta_{t_{z,p} t_{z,q}}}\langle pq|\mu|pq\rangle$$

Test of input M1 operator matrix elements

筑波大学 計算科学研究センター Center for Computational Sciences

NCSM vs Faddeev

R. Seutin et al., arXiv: 2308.00136.

NCSM requires the M1 operator, which can also be used in IMSRG calculations.

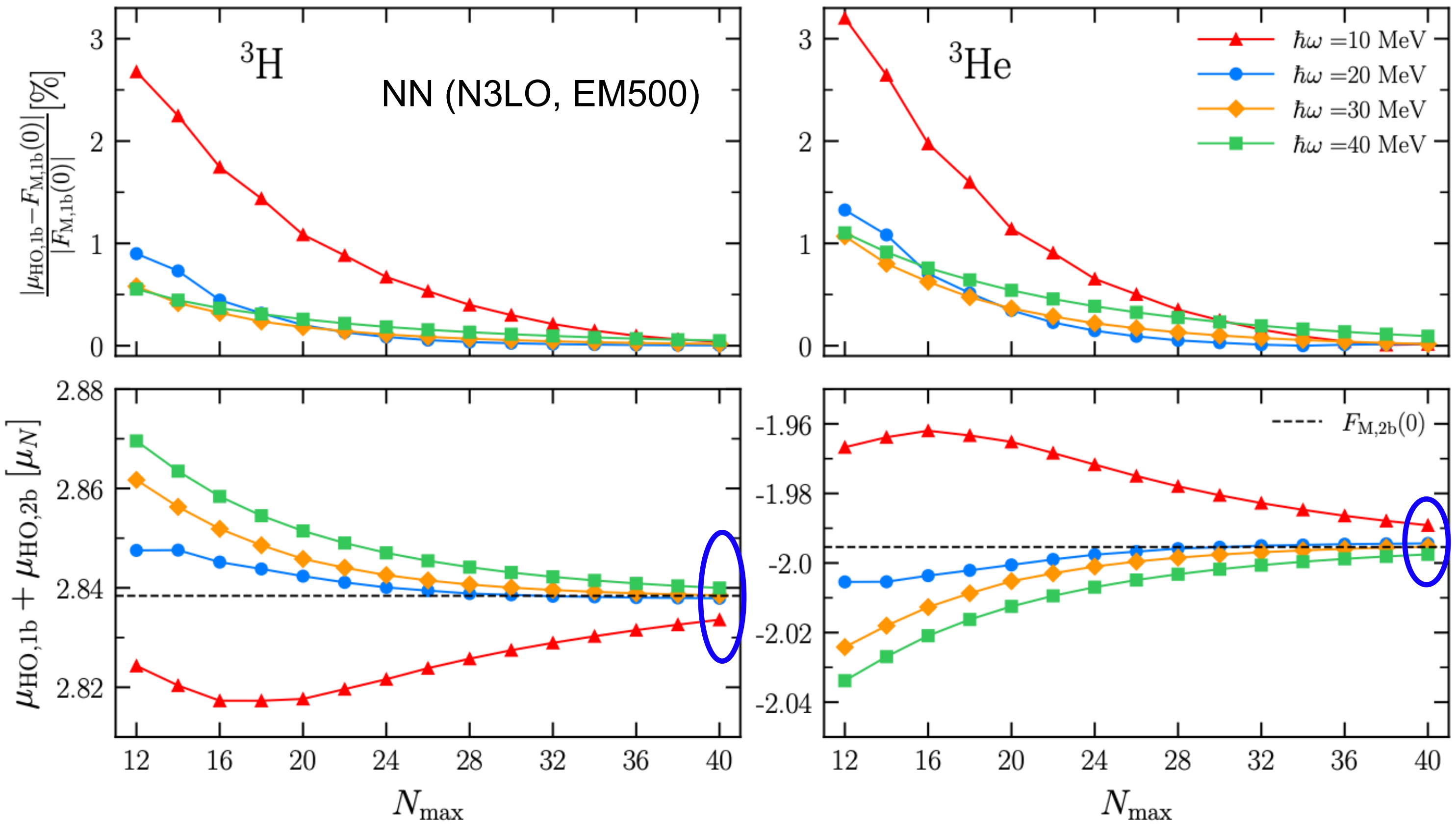

Faddeev results are obtained from the normalization of the magnetic form factor.

M1 matrix elements are correctly implemented!

Nuclear currents from chiral EFT

筑波大学 計算科学研究センター Center for Computational Sciences

Nuclear observables (EM properties, beta decay, …) are measured through the interaction between a nucleus and external field.

Chiral EFT allows us a systematic expansion for charge and current operators.

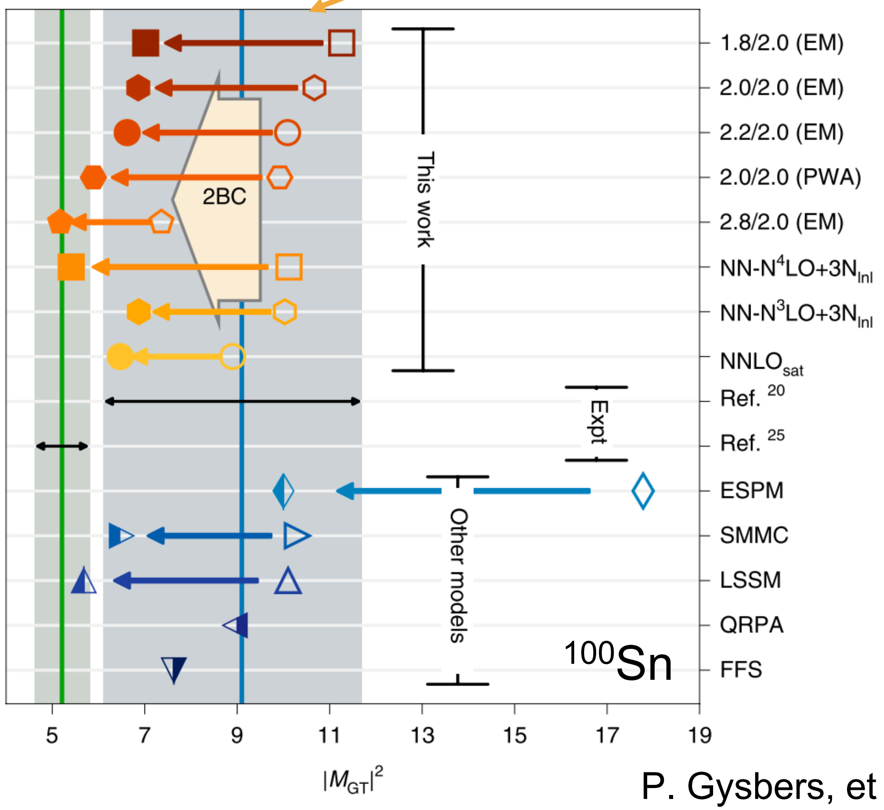

P. Gysbers, et al., Nat. Phys. 15, 428 (2019).

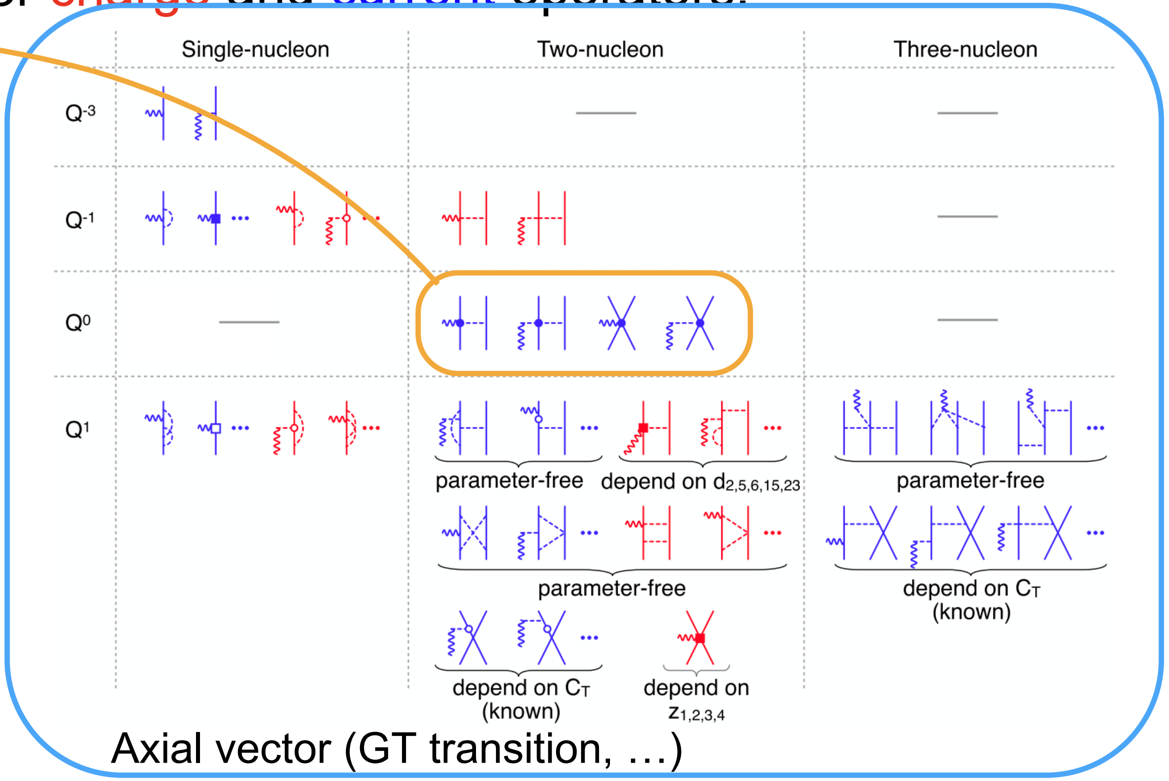

E. Epelbaum, arXiv:1908.09349.

Is ^{40}Ca magic?

2BC makes agreement worse.

Activating the ^{40}Ca core explains the magnetic moments better

The radii are not explained. Further investigations are needed!

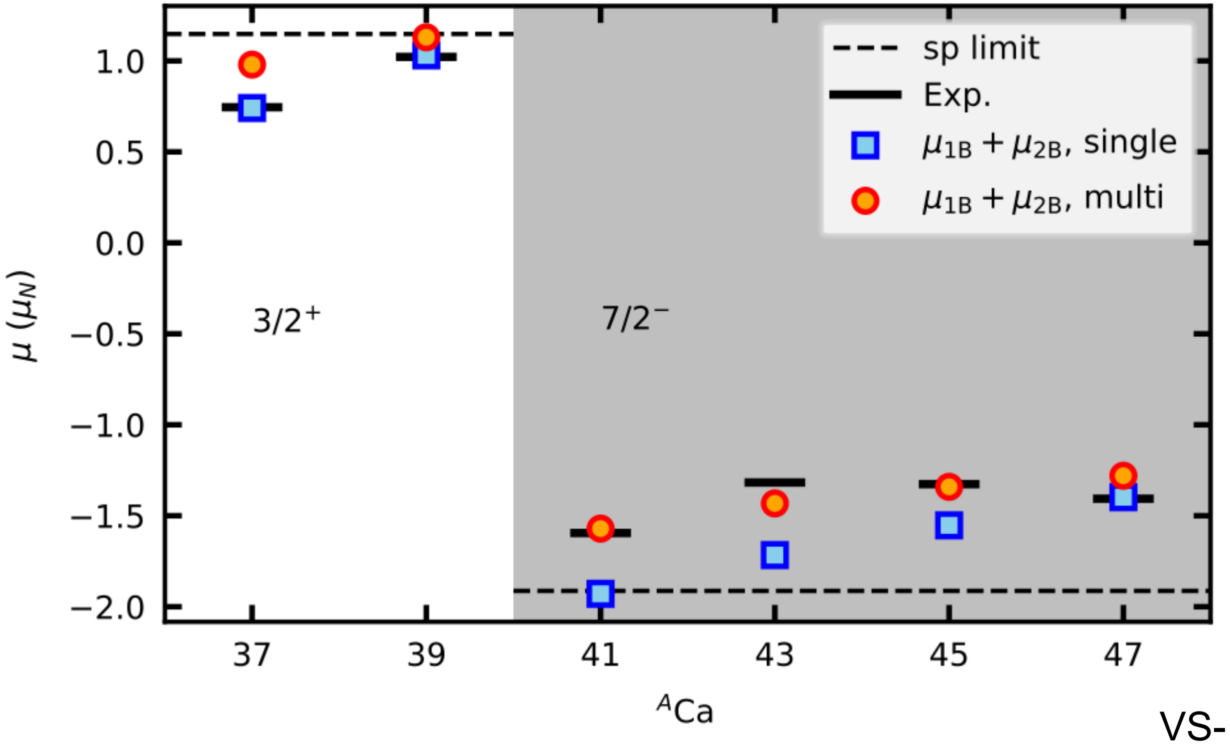

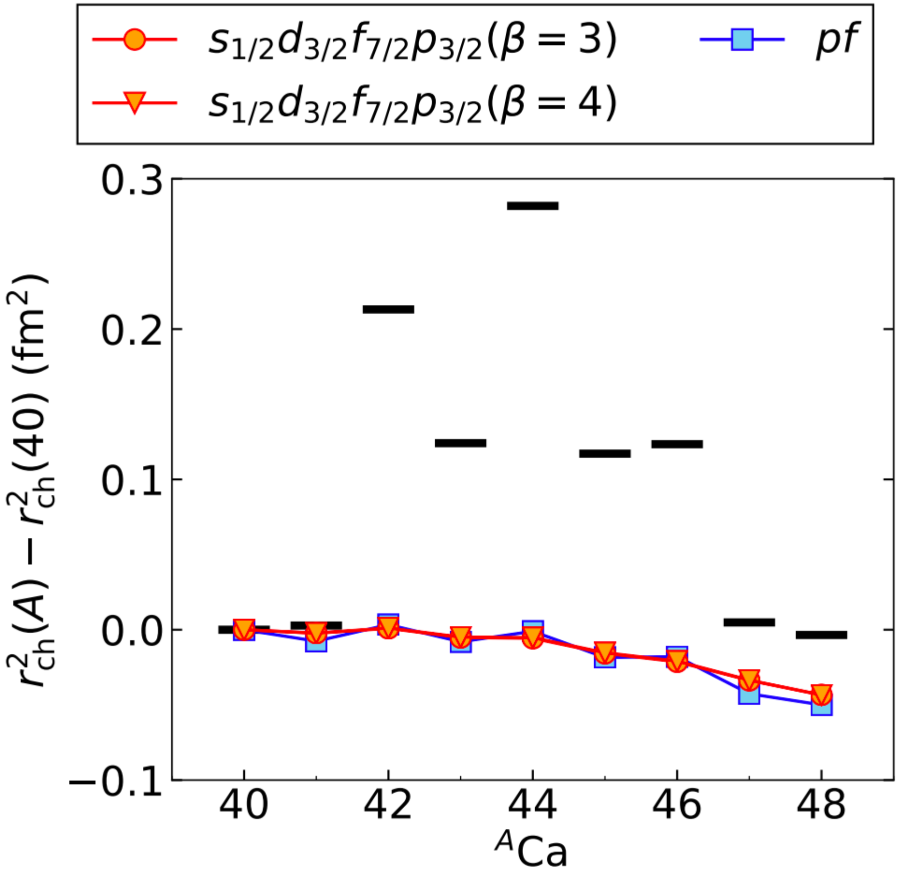

VS-IMSRG(2), 1.8/2.0 (EM)

TM et al., Phys. Rev. Lett. 132, 232503 (2024).

Mass dependence of 2B contribution

The size of 2BC contribution is larger in heavier systems.

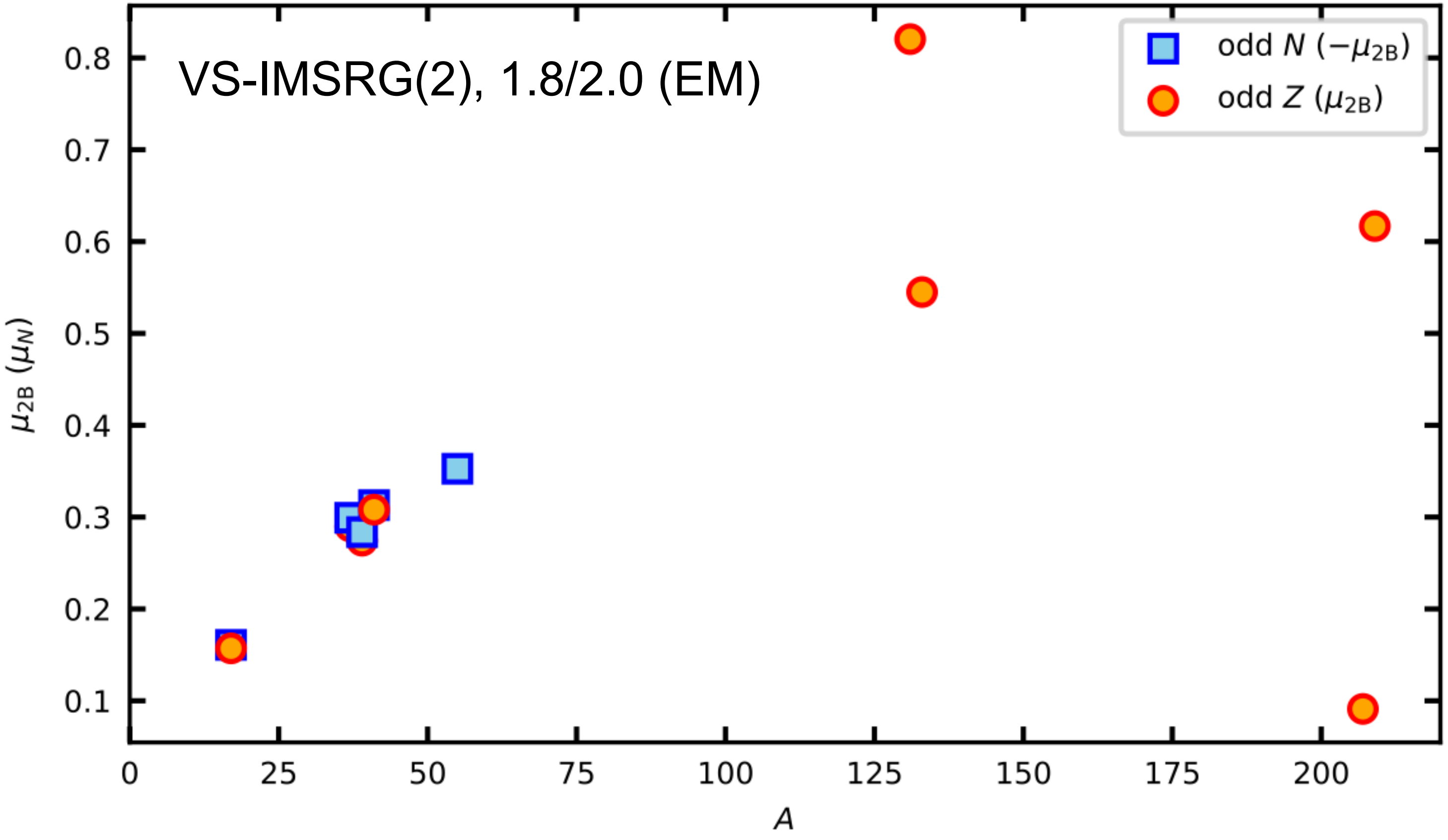

TM et al., Phys. Rev. Lett. 132, 232503 (2024).

Mass dependence of 2B contribution

The size of 2BC contribution is larger in heavier systems.

The simplest configuration limit is 0^+ core + 1 particle (or hole)

$$\langle J||\mu||J\rangle \sim \sum_{q\in\mathrm{core}}\sum_{I} f(j_p, j_q, I)\langle pq : I||\mu||pq : I\rangle$$

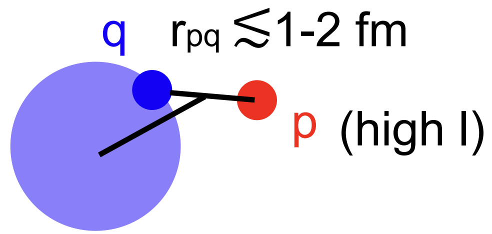

$R_{pq} \sim r_0A^{1/3}$

$$\boldsymbol{\mu}_{pq}^{\mathrm{Sachs}} \propto (\boldsymbol{R}_{pq}\times\boldsymbol{r}_{pq})V^{\pi}(r_{pq})$$

|r r| ≲ 1-2 fm because of pion exchange potential

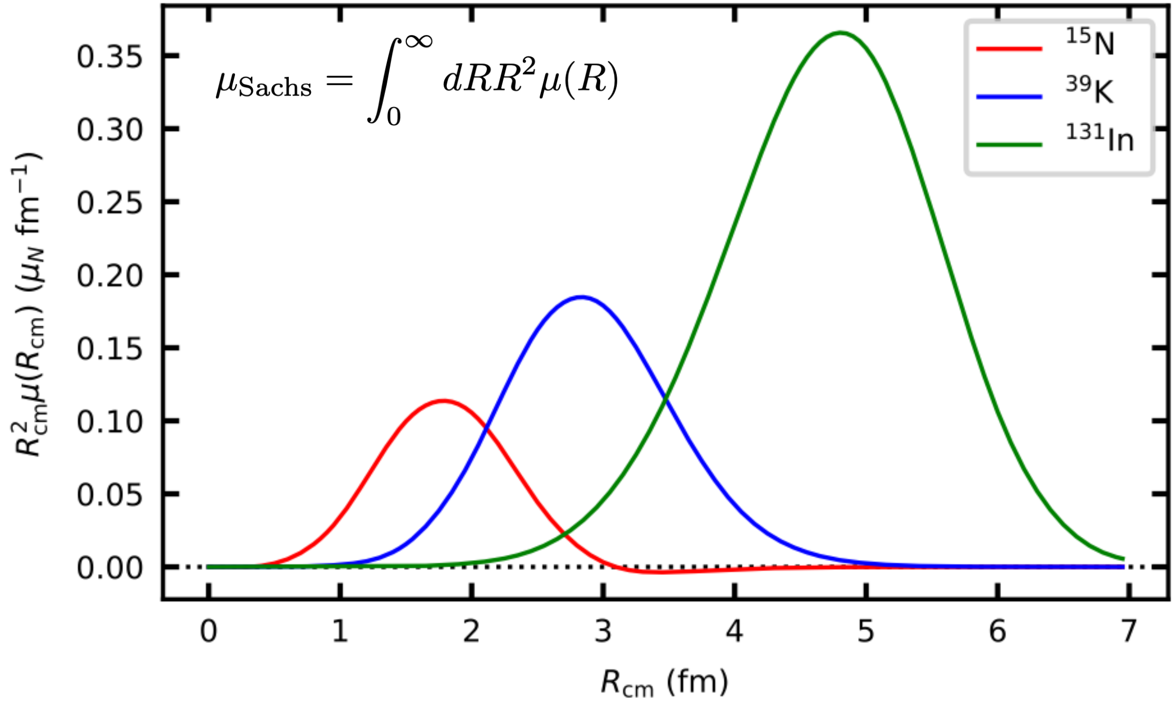

The peak position moves to larger R for heavier systems.

TM et al., Phys. Rev. Lett. 132, 232503 (2024).

4th moment of charge density

See also:
H. Kurasawa and T. Suzuki, Prog. Theor. Exp. Phys., 113D01 (2019).
H. Kurasawa and T. Suzuki, Prog. Theor. Exp. Phys., 013D02 (2020).
T. Suzuki, R. Danjo, T. Suda, Prog. Theor. Exp. Phys., 093D02 (2024).

In M. Door et al., arXiv:2403.07792, only the R_p^4 was computed.

4th moment of charge density: $$R_{\mathrm{ch}}^4 = \frac{60}{F_{\mathrm{ch}}(0)} \lim_{q\to 0} \frac{d}{dq^2}\frac{d}{dq^2} F_{\mathrm{ch}}(q).$$

Charge form factor: $$F_{\mathrm{ch}}(q) = e\sum_{i=1}^{A}\left\{G_i^E(q^2)\left[1-\frac{q^2}{8m^2}\right]j_0(x_i) - \frac{q^2}{2m^2}\left[G_i^M(q^2)-\frac{1}{2}G_i^E(q^2)\right](\boldsymbol{\ell}_i\cdot\boldsymbol{\sigma}_i)\frac{j_1(x_i)}{x_i}\right\},$$

$x_i = q|\boldsymbol{r}_i - \boldsymbol{R}_{\mathrm{cm}}|$ G^E and G^M are Sachs form factors

R_{ch}^4: $$R_{\mathrm{ch}}^4 = R_p^4 + \frac{10}{3}\left(r_p^2R_p^2 + \frac{N}{Z}r_n^2R_n^2\right) + \frac{5}{2m^2}\left(R_p^2 + r_p^2 + \frac{N}{Z}r_n^2\right) + r_p^4 + \frac{N}{Z}r_n^4 + R_{\mathrm{SO}}^4$$

$$R_p^2 = \frac{1}{Z}\sum_{i=1}^{A}\left(\frac{1+\tau_i}{2}\right)|\boldsymbol{r}_i - \boldsymbol{R}_{\mathrm{cm}}|^2,$$

$$R_n^2 = \frac{1}{N}\sum_{i=1}^{A}\left(\frac{1-\tau_i}{2}\right)|\boldsymbol{r}_i - \boldsymbol{R}_{\mathrm{cm}}|^2,$$

$$R_p^4 = \frac{1}{Z}\sum_{i=1}^{A}\left(\frac{1+\tau_i}{2}\right)|\boldsymbol{r}_i - \boldsymbol{R}_{\mathrm{cm}}|^4,$$

$$R_{\mathrm{SO}}^4 = \frac{2}{m^2Z}\sum_{i=1}^{A}\left[\left(\frac{1+\tau_i}{2}\right)\left(\mu_p - \frac{1}{2}\right) + \left(\frac{1-\tau_i}{2}\right)\mu_n\right](\boldsymbol{\ell}_i\cdot\boldsymbol{\sigma}_i)|\boldsymbol{r}_i - \boldsymbol{R}_{\mathrm{cm}}|^2$$
$$+\frac{10}{3m^2Z}\sum_{i=1}^{A}\left[\left(\frac{1+\tau_i}{2}\right)\left(r_{M,p}^2 - \frac{r_p^2}{2}\right) + \left(\frac{1-\tau_i}{2}\right)\left(r_{M,n}^2 - \frac{r_n^2}{2}\right)\right](\boldsymbol{\ell}_i\cdot\boldsymbol{\sigma}_i),$$